© 2019. Published by The Company of Biologists Ltd | Development (2019) 146, dev171298. doi:10.1242/dev.171298

RESEARCH ARTICLE

# A TOR-YAK1 signaling axis controls cell cycle, meristem activity and plant growth in *Arabidopsis*

**Adam Barrada[1,*], Meriem Djendli[1], Thierry Desnos[2], Raphael Mercier[3], Christophe Robaglia[1], Marie-Hélène Montané[1,‡] and Benoît Menand[1,‡]**

## ABSTRACT

TARGET OF RAPAMYCIN (TOR) is a conserved eukaryotic phosphatidylinositol-3-kinase-related kinase that plays a major role in regulating growth and metabolism in response to environment in plants. We performed a genetic screen for *Arabidopsis* ethylmethane sulfonate mutants resistant to the ATP-competitive TOR inhibitor AZD-8055 to identify new components of the plant TOR pathway. We found that loss-of-function mutants of the DYRK (dual specificity tyrosine phosphorylation regulated kinase)/YAK1 kinase are resistant to AZD-8055 and, reciprocally, that YAK1 overexpressors are hypersensitive to AZD-8055. Significantly, these phenotypes were conditional on TOR inhibition, positioning YAK1 activity downstream of TOR. We further show that the ATP-competitive DYRK1A inhibitor pINDY phenocopies *YAK1* loss of function. Microscopy analysis revealed that YAK1 functions to repress meristem size and induce differentiation. We show that YAK1 represses cyclin expression in the different zones of the root meristem and that YAK1 is essential for TOR-dependent transcriptional regulation of the plant-specific SIAMESE-RELATED (SMR) cyclin-dependent kinase inhibitors in both meristematic and differentiating root cells. Thus, YAK1 is a major regulator of meristem activity and cell differentiation downstream of TOR.

**KEY WORDS: Meristem, Differentiation, TOR, YAK1, DYRK, SMR**

## INTRODUCTION

Plant cells are produced in meristems, activity of which is controlled by hormones and environmental cues. During plant growth, cells originating from the stem cell niche divide inside the meristem before rapid expansion, and will acquire their final size and differentiation state according to the developmental program. Recent studies have shown that the TOR kinase plays an essential role in plant growth regulation by controlling cell proliferation and differentiation in meristems (Montane and Menand, 2013; Ren et al., 2012; Xiong et al., 2013). TOR belongs to the small phosphatidylinositol-3-kinase-related-kinases family (PIKKs), and is at the center of a major conserved eukaryotic signaling pathway that regulates growth and metabolism (Ben-Sahra and Manning, 2017; Gonzalez and Rallis, 2017; Loewith and Hall, 2011; van Dam et al., 2011). In *Arabidopsis*, the TOR pathway is activated by nutrients and by environmental and hormonal inputs, such as sucrose, light and auxin (Li et al., 2017; Schepetilnikov et al., 2017; Xiong et al., 2013). TOR regulates plant metabolism and therefore cell wall structure as well as cell contents, such as lipids, starch and amino acids (Caldana et al., 2013; Leiber et al., 2010; Moreau et al., 2012; Salem et al., 2017). TOR is also an essential regulator of cell proliferation in both root and shoot meristems (Li et al., 2017; Menand et al., 2002; Montane and Menand, 2013; Pfeiffer et al., 2016; Xiong et al., 2013). Several targets of *Arabidopsis* TOR have been identified, including the E2FA and E2FB transcription factors (Li et al., 2017; Xiong et al., 2013), the ribosomal protein S6 kinases (S6Ks) (Mahfouz et al., 2006; Xiong and Sheen, 2012) and the protein phosphatase PP2A (Ahn et al., 2011, 2015). However, their physiological contribution to TOR-mediated growth processes has not been fully determined.

We designed a pharmacogenetic approach to uncover new members of the plant TOR signaling pathway in plant growth regulation. We focused on primary root growth because it is a convenient system for studying the spatiotemporal dynamics of tissue and organ growth (Barrada et al., 2015). An ethylmethane sulfonate (EMS) *Arabidopsis* mutant collection was screened for plants resistant to the specific ATP-competitive TOR inhibitor AZD-8055 (Chresta et al., 2010), previously shown to be potent in plants (Dobrenel et al., 2016; Dong et al., 2015; Kravchenko et al., 2015; Li et al., 2015; Montane and Menand, 2013; Ouibrahim et al., 2015; Pfeiffer et al., 2016; Pu et al., 2017; Schepetilnikov et al., 2017; Zhang et al., 2016). This allowed us to identify three allelic mutants for which the phenotype was conditional to TOR inhibition. The gene responsible encodes a member of the DYRK (dual specificity tyrosine phosphorylation regulated kinase) family (Aranda et al., 2011), AtDYRK1A (Karpov et al., 2014) also named AtYAK1 (YET ANOTHER KINASE 1, named hereafter YAK1), which was previously reported to participate in abscisic acid (ABA) response and to optimize light-regulated growth in *Arabidopsis* (Huang et al., 2017; Kim et al., 2015). We found that loss-of-function mutations in *Arabidopsis YAK1*, as well as ATP-competitive DYRK1A inhibitors, prevent and partially rescue, respectively, the root growth inhibition and meristem downsizing induced by TOR inhibition. Reciprocally, YAK1 overexpression leads to the opposite phenotypes. Our data indicate that TOR regulates meristem activity via YAK1-dependent control of cell cycle regulators. We further show that YAK1 is essential for the TOR-dependent regulation of SIAMESE-RELATED (SMR) cyclin-dependent kinase (CDK) inhibitors.

[1]Aix Marseille Université, CEA, CNRS, BIAM, Laboratoire de Génétique et Biophysique des Plantes, Marseille, France F-13009. [2]Aix Marseille Univ, CEA, CNRS, BIAM, Laboratoire de Biologie du Développement des Plantes, Saint Paul-Lez-Durance, France F-13108. [3]Institut Jean-Pierre Bourgin (IJPB), Institut National de la Recherche Agronomique, AgroParisTech, CNRS, Université Paris-Saclay, 78000 Versailles, France.
*Present address: Pavillon Envirotron (EVT), Université Laval Québec, 2480 Boulevard Hochelaga, G1V 0A6, Québec, Canada.

‡Authors for correspondence (marie-helene.montane@univ-amu.fr; benoit.menand@univ-amu.fr)

M.D., 0000-0002-9466-4443; R.M., 0000-0001-6508-6608; M.-H.M., 0000-0001-9186-3802; B.M., 0000-0001-9713-5275

**Received 24 August 2018; Accepted 14 January 2019**

Development (2019) 146, dev171298. doi:10.1242/dev.171298

## RESULTS

### Mutations in the *YAK1* gene cause resistance to the TOR inhibitor AZD-8055

To find new genes involved in TOR-mediated growth regulation, ~$1.1\times10^5$ M2 seedlings from an EMS-mutagenized *Arabidopsis* Col$^{er105}$ library were screened for plants resistant to 1 µM AZD-8055, a concentration that causes 90% growth inhibition (GI) of the wild type (WT) (GI=90%) (Montane and Menand, 2013). After a two-step screen of M2 and M3 plants (see Materials and Methods), we isolated seven resistant mutants for which the primary roots were at least twice as long as that of the WT when grown on AZD-8055. The genome of the M3 progeny of each of these mutants was then sequenced, revealing that three mutants carried non-synonymous mutations in the *YAK1* genomic sequence (At5g35980) (Fig. 1A). Because *yak1* loss-of-function T-DNA insertion mutants have previously been reported (*yak1-1*, *yak1-2* and *yak1-3*; Huang et al., 2017; Kim et al., 2015), the new alleles were named *yak1-4*, *yak1-5* and *yak1-6* and a new loss-of-function T-DNA mutant was named *yak1-7* (Fig. 1A,B). The development of the aerial parts of the plant as well as the root was less affected by AZD-8055 in *yak1* mutants regardless of the accession (Fig. 1B). These results show that *yak1* mutations affect all vegetative growth, as does AZD-8055-mediated TOR inhibition (Montane and Menand, 2013).

To determine whether AZD-8055 resistance was of a dominant or recessive nature, the mutants were backcrossed to the WT, the F1 was selfed and the segregating F2 generation was scored for resistance to AZD-8055. The F2 progeny segregated in a ratio of one AZD-8055 resistant (GI=40-70%) to three sensitive (GI=85-95%) indicating that AZD-8055 resistance is a recessive trait in these mutants (Table S1). Genotyping of F2 plants grown on AZD-8055 showed that *yak1* homozygous mutations segregate with AZD-8055 resistance (Table S2). Allelism tests confirmed the causal relationship between mutations in the *YAK1* genomic sequence and AZD-8055 resistance (Fig. S1). Each *yak1* EMS mutant has one (*yak1-5* and *yak1-6*) or two (*yak1-4*) mutations in different highly conserved motifs of the catalytic domain of YAK1/DYRK1A

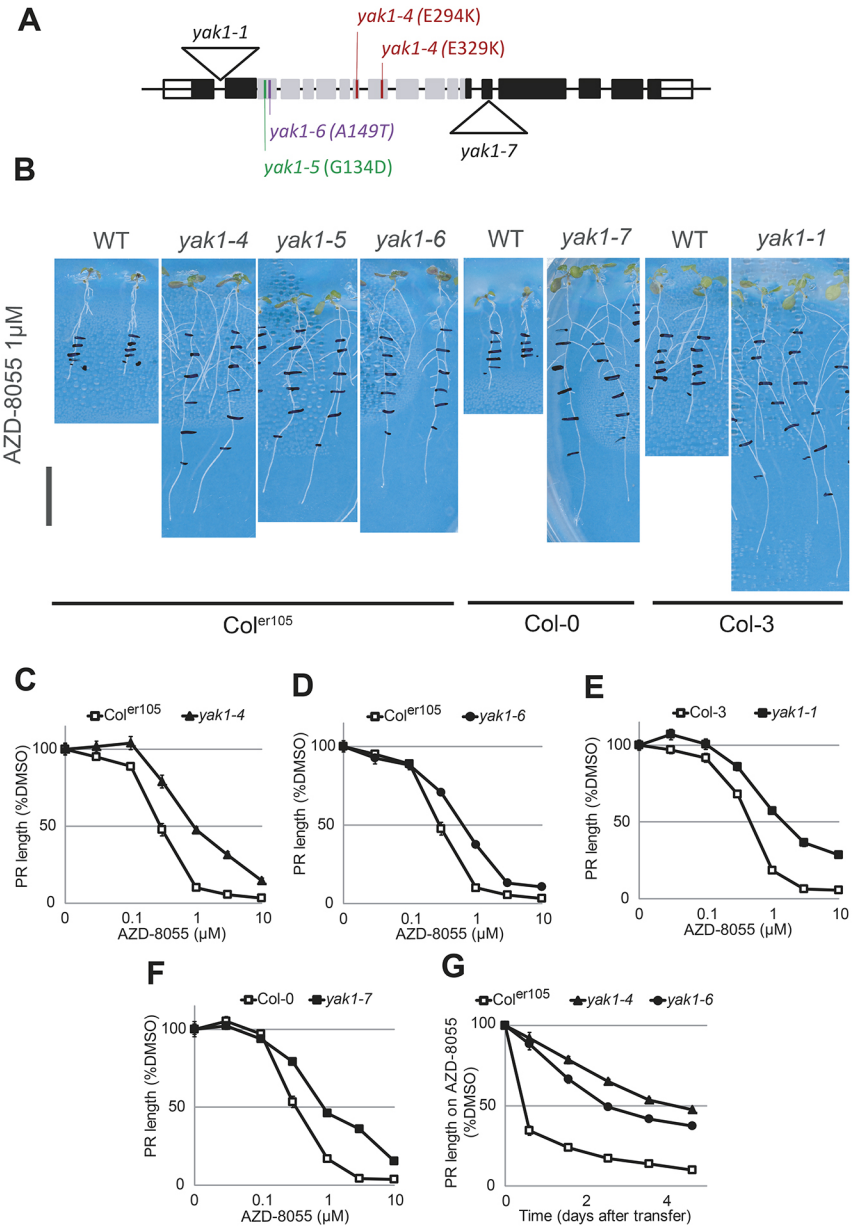


**Fig. 1. Mutations in *YAK1* suppress AZD-8055-mediated primary root (PR) growth inhibition.** (A) Position and nature of *yak1* mutations used in this study. The predicted catalytic domain is in gray. (B) Images of WT and *yak1* mutants in different accessions 7 days after transfer to 1 µM AZD-8055. Scale bar: 1 cm. (C-F) AZD-8055 dose-response curves of EMS mutants and T-DNA insertion lines and respective WT accessions 5 days after transfer to drug-containing media. (G) Time course of root growth delay of EMS mutants after transfer to 1 µM AZD-8055. Root length is presented as a percentage of WT root length on DMSO (*n*=14-16).

Development (2019) 146, dev171298. doi:10.1242/dev.171298

(Fig. 1A, Fig. S2). Substitution of amino acids close to the mutation sites of *yak1-4* and *yak1-5* have been shown to reduce human DYRK1A activity (Wiechmann et al., 2003). Furthermore, *yak1-6* has a mutation in a conserved glycine of the ATP-anchor motif which substitution leads to loss of activity in the human insulin receptor tyrosine kinase (Odawara et al., 1989). This suggests that YAK1 function is impaired in these mutants. In agreement with this hypothesis, analysis with Meta-SNP (Capriotti et al., 2013), a program that predicts whether a mutated amino acid will affect protein function, showed that all amino acid substitutions were non-neutral and should alter YAK1 activity (Table S3).

Dose-response curves were generated to determine whether the different *yak1* mutants showed comparable responses at different AZD-8055 concentrations. The AZD-8055 dose response curves of *yak1* EMS mutants (Fig. 1C,D) as well as of *yak1* T-DNA KO insertion mutants (Fig. 1E,F) were similarly shifted towards higher AZD-8055 concentrations compared with the WT. This confirmed that EMS mutants were likely loss-of-function mutants. Noticeably, in most cases, the difference between the mutant and the WT increased at higher AZD-8055 concentrations confirming the TOR inhibition-dependent phenotype. Time-course experiments also showed that mutations in *yak1* oppose AZD-8055-triggered growth reduction during the first 12 h after transfer onto AZD-8055 (Fig. 1G). Moreover, the morphology of *yak1* mutants was similar to the WT without drug (Fig. S3). Together, these data show that YAK1 is a repressor of growth, and its function is conditional upon TOR inactivation, indicating that it acts downstream of TOR.

### YAK1 chemical inhibitors phenocopy *yak1* loss-of-function mutations

*Arabidopsis* YAK1 was previously reported as the homolog of human/*Drosophila* DYRK1A/Minibrain (Aranda et al., 2011; Karpov et al., 2014), an essential regulator of cell cycle exit in the central nervous system and a contributor to Down syndrome (Najas et al., 2015; Soppa et al., 2014). ATP competitive DYRK1A inhibitors have been developed to study the role of DYRK1A in brain cell proliferation and development (Ogawa et al., 2010; Wang et al., 2015). Sequence alignment shows that the catalytic domain is highly conserved between *Arabidopsis* YAK1 and human DYRK1A (Fig. S2). In addition, the residues in DYRK1A that are critical for the binding of ATP-competitive DYRK1A inhibitors (Ogawa et al., 2010) are also conserved in *Arabidopsis* YAK1. This suggested that DYRK1A inhibitors would also inhibit *Arabidopsis* YAK1. To test this hypothesis, the effect of two ATP-competitive DYRK1A inhibitors, INDY and its more lipophilic prodrug proINDY (pINDY) was investigated on the WT Col-0 accession. Both INDY and pINDY had no clear-cut effect on the root length of plants grown on standard medium (Fig. 2A). However, INDY and pINDY partially restored the root growth of WT plants inhibited by 1 µM AZD-8055 (Fig. 2B, Fig. S4A). The growth restoration process was INDY/pINDY dose dependent and reduced WT growth inhibition from GI ∼90% to up to GI ∼75% (Fig. 2B). The phenotype of WT seedlings treated with AZD-8055 and pINDY was similar to that of *yak1-7* treated with AZD-8055 showing that pINDY treatment phenocopies *yak1* loss-of-function mutations (Fig. S4A). pINDY treatment had no effect on homozygous *yak1* mutants grown without AZD-8055 (Fig. S4B) and hardly restored their growth upon AZD-8055 treatment (Fig. 2C). This confirmed that the effect of pINDY on root length restoration is YAK1 dependent. Because pINDY promoted a slightly better root growth recovery than INDY and there was no big increase in growth between 20 and 40 µM, pINDY was used thereafter at 20 µM (Fig. 2C, Fig. S4A), a concentration that is close to those used in human cell cultures (Ogawa et al., 2010; Seu et al., 2015; Wang et al., 2015).

In order to confirm that the YAK1 loss-of-function phenotype was independent of the class of drugs inhibiting TOR, we tested the sensitivity of *yak1* mutants and pINDY-treated WT plants to the allosteric inhibitor rapamycin and to WYE-132, another ATP-competitive TOR inhibitor that is highly selective over PI3Ks and other PIKKs (Yu et al., 2010) and was reported to be effective in plants (Montane and Menand, 2013). *yak1* mutants were less sensitive to WYE-132 than WT (Fig. 2D) and pINDY partially restored WT root growth (Fig. 2E) showing that the *yak1* mutant phenotype and the effect of pINDY were independent of the nature of the ATP-competitive TOR inhibitor. Similarly, pINDY partially restored growth on rapamycin of BP12-2 plants, which overexpress the yeast FKBP12 (12 kDa FK506-binding protein) necessary for the formation of the FKBP12-rapamycin-TOR inhibitory complex (Ren et al., 2012) (Fig. 2F). In contrast, *yak1* mutants were as sensitive as the WT to roscovitin (Fig. S5), an ATP-competitive CDK inhibitor (Meijer et al., 1997) that inhibits root growth via a different mechanism than do TOR inhibitors in *Arabidopsis* (Montane and Menand, 2013), highlighting the specificity of the phenotype towards TOR inhibition. Overall, this showed that the partial restoration of growth by pINDY is independent of the nature of the TOR inhibitor, and confirms that the *yak1*- and pINDY-dependent phenotypes are indeed conditional on TOR inhibition.

### Meristem size reduction upon TOR inhibition requires YAK1

Root length is determined by cell proliferation in the meristem and cell expansion during differentiation. During this process, the control of the number of dividing cells is of primary importance (Beemster and Baskin, 1998; Sugimoto-Shirasu and Roberts, 2003). TOR inhibition was previously reported to decrease the size of the division zone and to concomitantly induce early differentiation (Montane and Menand, 2013; Ren et al., 2012; Xiong et al., 2013). To investigate the role of YAK1 in these processes, we first focused on the size of the meristematic zone (MZ) defined as the distance from the quiescent center (QC) up to the first rapidly elongating cortical cell, corresponding to the transition zone (TZ) (Perilli and Sabatini, 2010). Differential interference contrast (DIC) microscopy images showed that EMS *yak1* mutants (Fig. 3A,B) as well as T-DNA mutants (Fig. 3C,D, Fig. S6) had an MZ that was a similar size to that of the WT when grown on DMSO, but larger than the WT in the presence of AZD-8055. Although pINDY alone had no effect on the WT MZ on standard medium, it restored the MZ in plants treated with AZD-8055 (Fig. 3C) to a size similar to that of *yak1* mutants grown on AZD-8055 (Fig. 3D). The larger MZ of *yak1-7* in the presence of AZD-8055 was associated with an increase from ∼20 to 30 cortical cells compared with WT, indicating that YAK1 controls the number of dividing cells (Fig. S7A). In addition, the differentiated epidermal cells of *yak1* mutants grown on AZD-8055 and of WT in the presence of pINDY and AZD-8055 were longer than those of WT grown on AZD-8055 (Fig. S8). This is consistent with the opposite phenotype of TOR-inhibited roots that showed decreased epidermal cell elongation as the MZ was reduced (Montane and Menand, 2013). These results show that YAK1 acts on both cell proliferation and cell expansion.

The production of plants carrying the *YAK1* promoter and *YAK1* coding region fused to the *GUS* (β-glucuronidase) reporter (*pYAK1::YAK1-GUS*) allowed us to isolate lines expressing different levels of the chimeric YAK1-GUS protein (Fig. S9A,B).

Development (2019) 146, dev171298. doi:10.1242/dev.171298

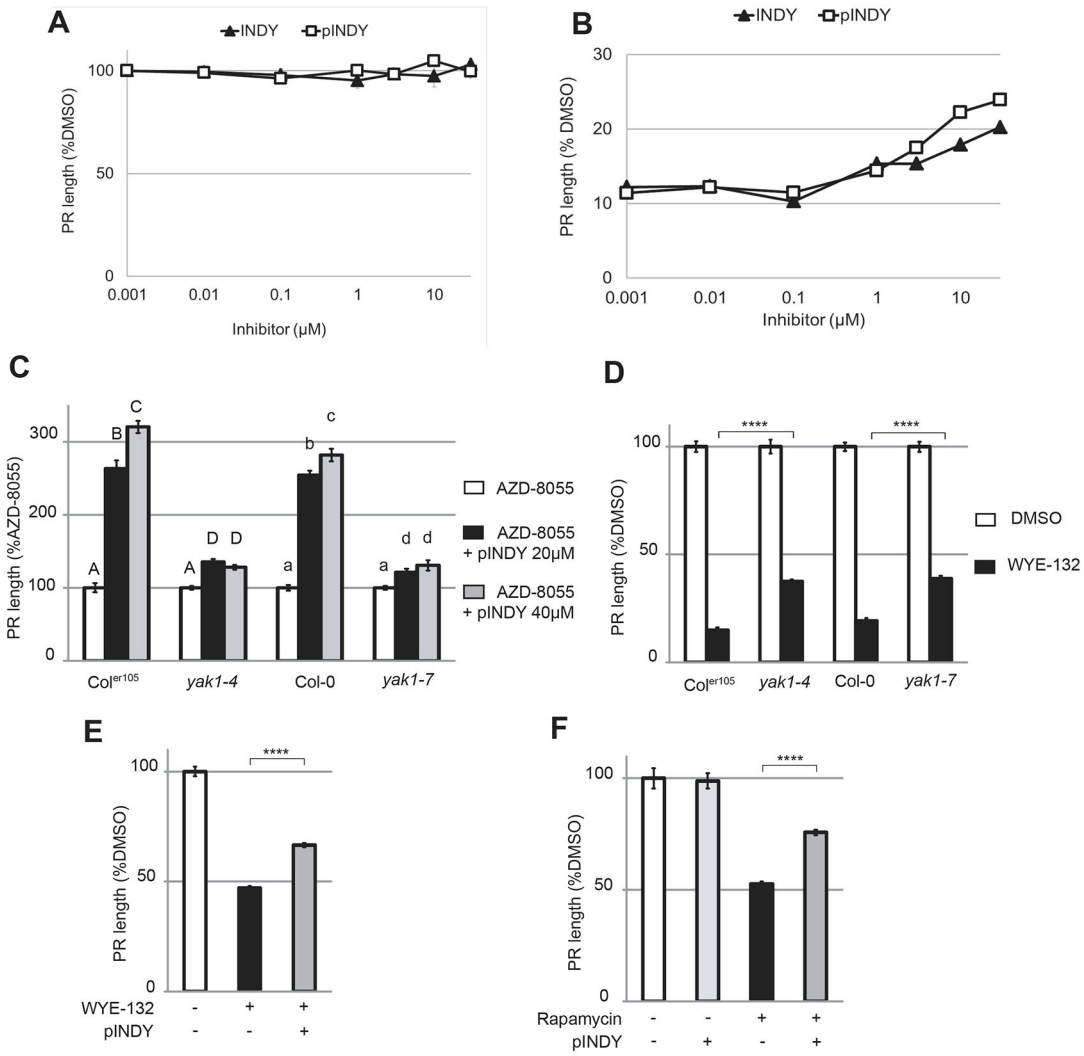


**Fig. 2. The ATP-competitive DYRK1A inhibitor pINDY phenocopies the resistance of *yak1* mutants to different TOR inhibitors.** Primary root (PR) length was measured 5 days after transfer to drug-containing media and is expressed as a percentage of the length on DMSO unless otherwise stated. (A,B) Dose-dependent effect of INDY and pINDY on WT Col-0 root grown without (A) or with (B) AZD-8055 (1 µM) ($n$=15-24). (C) Root growth of *yak1* mutants and WT accessions grown on 1 µM AZD-8055 alone or in combination with pINDY. Root length is expressed as a percentage of root length on AZD-8055 ($n$=8-27, two-way ANOVA, $P$<0.05, two separate tests: uppercase letters for *yak1-4* versus Col$^{er105}$ and lowercase letters for *yak1-7* versus Col-0). (D) Root growth of *yak1* mutants and WT accessions grown on 0.2 µM WYE-132 ($n$=16, two-tailed Student's $t$-test, ****$P$<0.0001). (E) Root growth of Col-0 plants grown on 0.2 µM WYE-132 alone or in combination with pINDY ($n$=31-32, two-tailed Student's $t$-test, ****$P$<0.0001). (F) Root growth of BP12-2 plants grown on 20 µM pINDY and/or 0.5 µM rapamycin ($n$=16, two-tailed Student's $t$-test, ****$P$<0.0001).

A line with high levels of YAK1-GUS expression, hereafter named *YAK1-GUS*$^{OE}$ (YAK1-GUS overexpressor) was investigated for altered sensitivity to pINDY and AZD-8055. *YAK1-GUS*$^{OE}$ root length and MZ size were similar to those of WT grown on DMSO (Fig. 3E,F, Fig. S9C). Strikingly, however, the sensitivity of *YAK1-GUS*$^{OE}$ to AZD-8055 was strongly increased: 0.4 µM AZD-8055 caused the same growth inhibition in *YAK1-GUS*$^{OE}$ as 1 µM AZD-8055 caused in the WT (Fig. 3E,F, Fig. S9C). This result shows that YAK1-GUS protein is functional in *YAK1-GUS*$^{OE}$ and is consistent with the hypothesis that YAK1 acts as a TOR inhibition-dependent growth repressor. At 1 µM AZD-8055, *YAK1-GUS*$^{OE}$ roots contained fewer MZ cells than the WT (Fig. S7B), and also displayed precocious protoxylem differentiation (Fig. 3E, Fig. S10). In addition, *YAK1-GUS*$^{OE}$ MZ size on AZD-8055 could be restored to a size close to the WT by the application of pINDY (Fig. 3E,F). Therefore, the MZ decrease in the *YAK1-GUS*$^{OE}$ and its reciprocal increase in *yak1* mutants, which are both conditional on TOR inhibition, demonstrate that YAK1 is a repressor of meristem activity that acts downstream of TOR.

### *YAK1* is expressed in the root meristem

Another *pYAK1::YAK1-GUS* line (Fig. S9B) showing lower levels of GUS expression than *YAK1-GUS*$^{OE}$, named hereafter *YAK1-GUS*$^{LE}$, was used to compare the expression patterns of YAK1 and TOR in root tips (Barrada et al., 2015; Menand et al., 2002) (Fig. 3G). On standard media, YAK1 and TOR proteins were both expressed in the MZ, suggesting that they might be present together within the same cells. This supports the idea that TOR could regulate YAK1 either directly or indirectly within the MZ. Interestingly, YAK1 was more widely expressed in the root tip than TOR (Barrada et al., 2015) with an expression zone that also included the root cap, the columella and beyond the TZ into the vascular cylinder (Fig. S9D). This suggests that the transcriptional expression of endogenous *YAK1* and *TOR* is differently regulated,

Development (2019) 146, dev171298. doi:10.1242/dev.171298

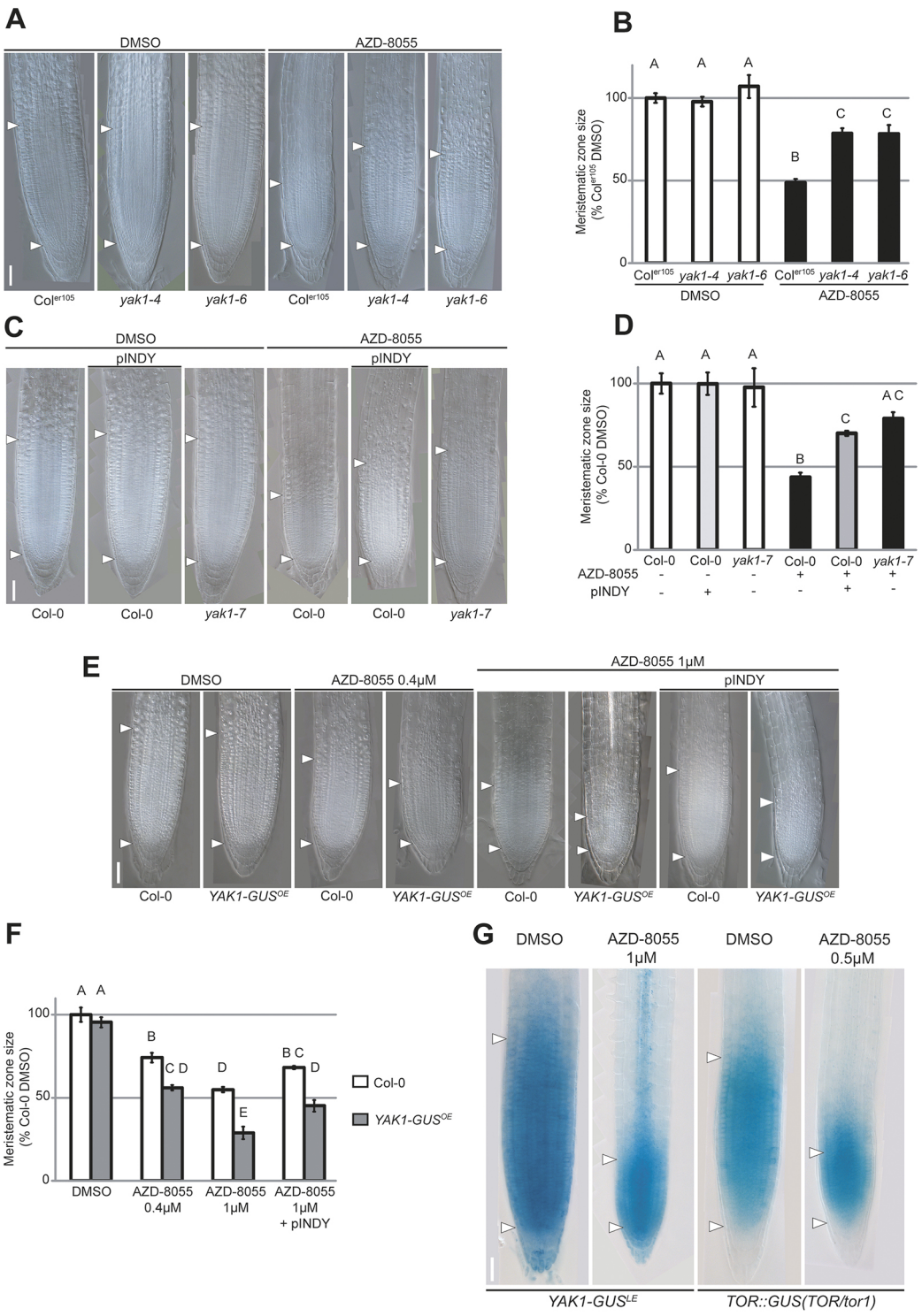


**Fig. 3. *YAK1* regulates root meristem activity.** Root meristems were analyzed 48 h after transfer to drug-containing medium. (A-D) Meristem phenotype of two EMS mutants (*yak1-4* and *yak1-6*) compared with Col$^{er105}$ grown on 1 µM AZD-8055 (A,B) and of a T-DNA line (*yak1-7*) and Col-0 grown on 1 µM AZD-8055, 20 µM pINDY or a combination of both drugs (C,D). (E,F) Meristem phenotype of *YAK1-GUS*$^{OE}$ compared with Col-0 grown on AZD-8055 alone or in combination with 20 µM pINDY. (A,C,E) DIC microscopy pictures of the MZ. (A,C,E,G) The lower and upper arrowheads highlight the QC and TZ, respectively. (B,D,F) The length of the MZ is expressed as a percentage of the size of the WT accession on DMSO ($n$=7-8, two-way ANOVA, $P$<0.05). (G) *pYAK1::YAK1-GUS* and *pTOR::TOR-GUS* expression profiles in the root tip in the presence of 1 µM and 0.5 µM AZD-8055, respectively. These AZD-8055 doses give similar levels of growth inhibition for each line because TOR::GUS is a heterozygous T-DNA mutant (Montane and Menand, 2013). Scale bars: 50 µm.

*TOR* being expressed mainly in the meristem whereas *YAK1* is expressed both in the meristem and in the vasculature above the MZ. Upon treatment with AZD-8055, this pattern is reinforced (Fig. 3G, Fig. S11) and is associated with a closer protoxylem (Fig. S11), suggesting that YAK1 expression might regulate the transition of cells from division to differentiation along the root.

Development (2019) 146, dev171298. doi:10.1242/dev.171298

### TOR inhibition perturbs expression of cell cycle genes in a YAK1-dependent manner

In concertation with development and hormonal patterns, cell proliferation occurs as a result of periodic activation of CDK by different cyclins (CYC), ensuring the transition from one phase of the mitotic cycle to another. To characterize further the effect of YAK1 on cell division, we investigated the patterns of a comprehensive panel of GUS transcriptional and translational reporter lines for cyclins. These lines are markers of the G1 and S phase (CYCA3 and CYCD) and the G2 and M phase (CYCA2 and CYCB). They are expressed in different root zones, i.e. the columella and procambium (CYCD3;3), the cortex and endodermis initials (CYCD6;1), the highly dividing meristem (CYCBs), and the TZ (CYCA2;3) (Bulankova et al., 2013; Collins et al., 2015; Forzani et al., 2014; Sozzani et al., 2010).

Treatment with AZD-8055 reduced the extent of GUS staining for most reporter lines, indicating a stringent decrease in cell cycle activity (Fig. 4A, Fig. S12). Indeed, the longitudinal reduction of expression of the proliferation-associated cyclins CYCBs and CYCA3s reflects a general downturn of cell cycling that is concomitant to the MZ reduction. Furthermore, *pCYCD6;1::GUS* expression nearly collapses after AZD-8055 treatment, suggesting a repression of the formative divisions. In contrast, *pCYCD3;3::GUS* intensity increased in the MZ, with reduced longitudinal expression and a strong concentration in the procambium. As CYCD3;3 is involved in secondary growth of the procambium (Collins et al.,

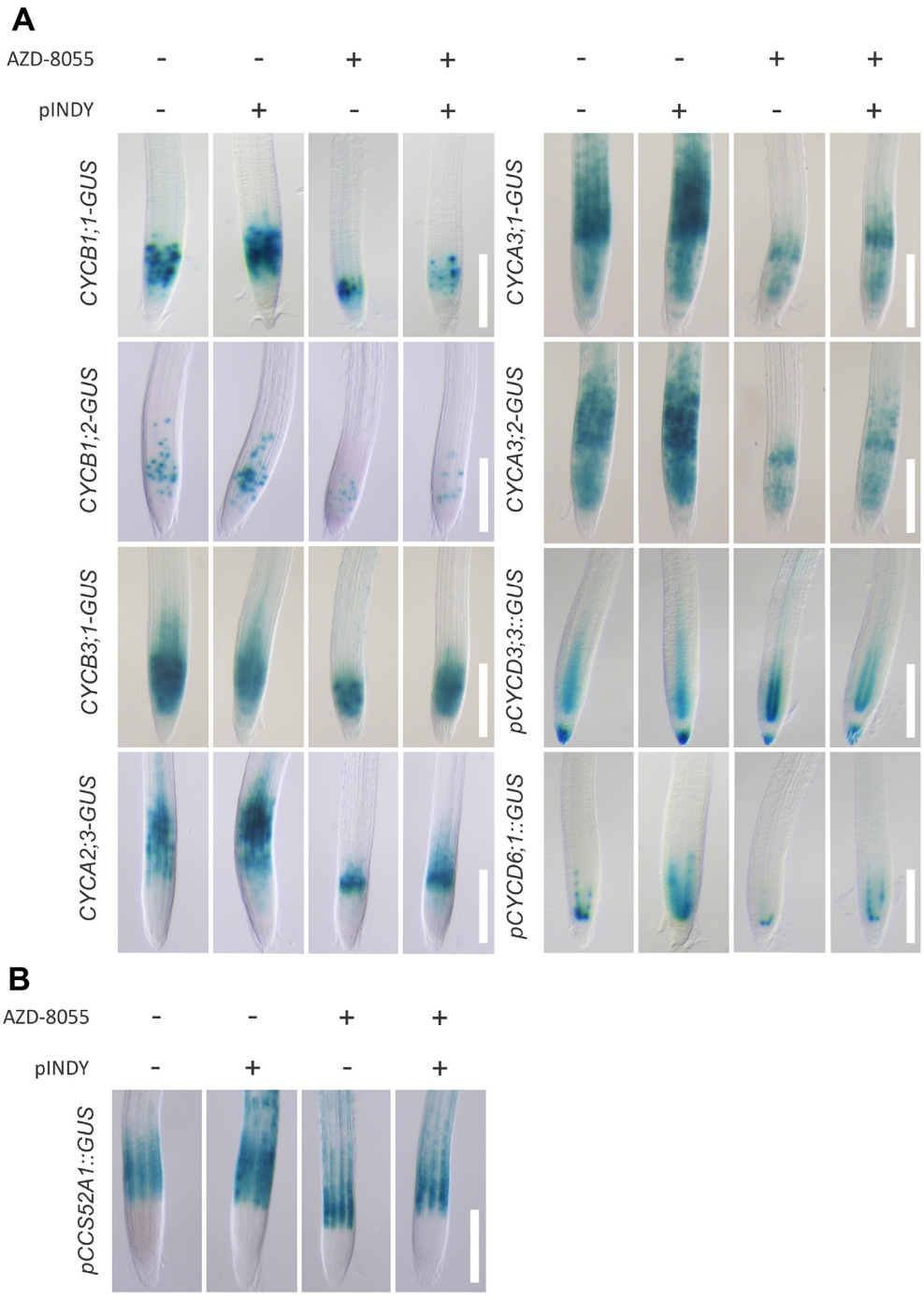


**Fig. 4. pINDY partially restores normal patterns of cell cycle marker expression in plants treated with AZD-8055.** GUS reporter lines were stained 48 h after treatment with 20 µM pINDY, 1 µM AZD-8055 or a combination of both. (A) Translational reporter lines *CYCB1;1-GUS*, *CYCB1;2-GUS*, *CYCB3;1-GUS*, *CYCA2;3-GUS*, *CYCA3;1-GUS* and *CYCA3;2-GUS*, and transcriptional reporter lines *pCYCD3;3::GUS* and *pCYCD6;1::GUS*. (B) Transcriptional reporter line *pCCS52A1::GUS*. Scale bars: 250 µm. A set of images for each condition and each marker is given in Fig. S12.

Development (2019) 146, dev171298. doi:10.1242/dev.171298

2015), this change suggests that there is an effect on procambium differentiation. This potential effect on vasculature development might be related to the high expression of YAK1-GUS in the stele in response to AZD-8055 (Fig. 3G). Meanwhile, AZD-8055 severely restricted *CYCA2.3-GUS* expression and shifted it towards the QC (Fig. 4B), suggesting a decrease in cells initiating endoreplication in the first steps of differentiation (Boudolf et al., 2009; Breuer et al., 2014; Imai et al., 2006). This is consistent with the concomitant shift of the marker of endoreplication *pCCS52A1::GUS* (CCS52A1, CELL CYCLE SWITCH PROTEIN 52 A1) (Breuer et al., 2014; De Veylder et al., 2011). Altogether, these patterns suggest that the transition of cells from mitosis to the onset of the endocycle occurs earlier when TOR is inhibited. Adding pINDY in combination with AZD-8055 partially restored the expression of CYCs and *CCS52A1* towards their DMSO patterns (Fig. 4A,B, Fig. S12), suggesting that YAK1 is a general regulator of the cell cycle. This is again consistent with the partial recovery of MZ size observed by DIC microscopy (Fig. 3C,D). Interestingly, treatment with pINDY alone, which does not change the length of the root or the meristem (Fig. 3D), slightly enhanced GUS staining intensity for cyclins involved in cell proliferation and formative divisions, particularly CYCB1;1, CYCD6;1 and CYCA2;3 (Fig. 4A). Although subtle, these changes are opposite to AZD-8055 effects and suggest that under standard growth conditions and in the absence of drug endogenous YAK1 might still have a small effect on proliferation. Altogether, our data illustrate how the balance between TOR and YAK1 activities might regulate the dynamics of root tip zone morphology through control of the overall cell cycle rate as well as the early steps of differentiation by a general modulation of CYC expression.

### TOR and YAK1 regulate the expression of SMR family CDK inhibitors

We showed above that TOR inhibition reduces the expression of CYCs, which are essential activators of CDKs. CYC-CDK activity is regulated by several mechanisms, including transcriptional regulation, proteolysis and interactions with CDK inhibitors. CDK inhibitors are crucial for plant development, particularly during the transition from the mitotic cell cycle to endoreplication (Breuer et al., 2014; De Veylder et al., 2011; Inagaki and Umeda, 2011). Considering the general repression of CYCs shown above, we aimed to study the expression of the plant-specific CDK inhibitors *SIAMESE* (*SIM*) and *SIAMESE-RELATED* (*SMR*), which can interact with and inhibit all CDKs (Churchman et al., 2006; De Veylder et al., 2011; Kumar et al., 2015; Van Leene et al., 2010). We used promoter-driven GUS reporter lines to study the expression of *SIM* and SMRs in roots (Fig. 5A, Fig. S13) (Yi et al., 2014). The marker of the elongation zone *pSIM::GUS* (Yi et al., 2014) was shifted towards the root tip by AZD-8055 similarly to *pCCS52A1::GUS* (Fig. 4B), suggesting again an early transition to endoreplication associated with the reduction of the MZ size. In contrast, *SMR4*, *SMR5* and *SMR7* GUS reporter lines showed the most remarkable responses. Their expression patterns were strongly enhanced upon AZD-8055 treatment, with *pSMR4::GUS* showing the most intense and extensive staining, encompassing dividing (*SMR4* and *SMR5*) as well as differentiating (*SMR4* and *SMR7*)

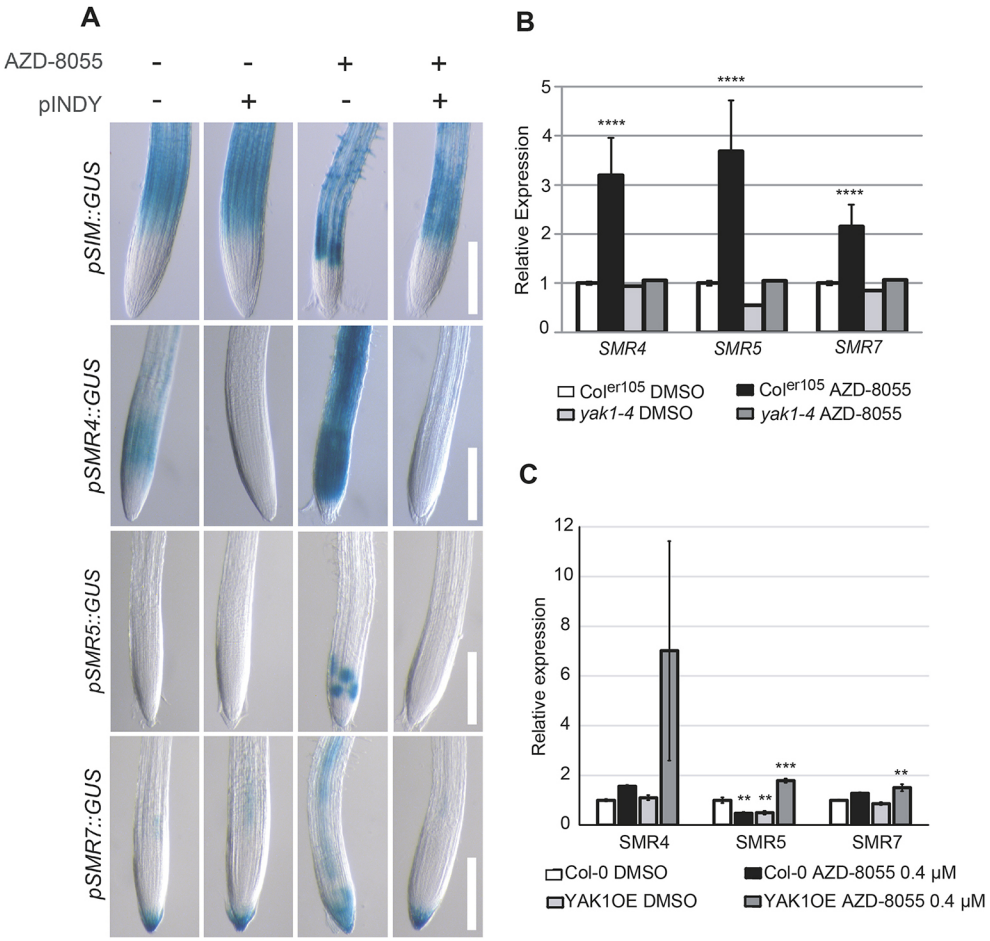


**Fig. 5. YAK1-dependent SMR transcription upon TOR inhibition.** (A) Transcriptional reporter lines *pSIM::GUS*, *pSMR4::GUS*, *pSMR5::GUS* and *pSMR7::GUS* stained 48 h after treatment with 20 µM pINDY, 1 µM AZD-8055 or a combination of both. Scale bars: 250 µm. A set of images for each condition and each marker is given in Fig. S13. (B,C) RT-qPCR analysis of the relative transcript level of *SMR4*, *SMR5* and *SMR7* after 48 h on 1 µM AZD-8055 in WT Col$^{er105}$ and the *yak1-4* EMS mutant (B) or on 0.4 µM AZD-8055 in WT Col-0 and *YAK1-GUS*$^{OE}$ (C). Expression levels are relative to Col$^{er105}$ or Col-0 grown on DMSO ($n$=3, two-way ANOVA, each condition compared with the control, $^{**}P<0.01$; $^{***}P<0.05$; $^{****}P<0.0001$).

Development (2019) 146, dev171298. doi:10.1242/dev.171298

zones of the root (Fig. 5A, Fig. S13). Remarkably, treatment with pINDY in combination with AZD-8055 either almost completely eliminated *pSMR::GUS* expression (*SMR4* and *SMR5*), or severely limited it (*SMR7*), showing that the transcription of all three SMRs appears to be dependent on YAK1 activity. Treatment with pINDY alone erased *pSMR4::GUS* expression, which overlaps part of MZ and the TZ on DMSO only. This suggests that YAK1 could have a basal level of activity when TOR is active in the MZ. This finding is also consistent with the enhanced CYC expression that we previously observed in the same zone in pINDY-treated plants (Fig. 4A) demonstrating a YAK1-dependent, inverse regulation of CYCs and SMRs. Interestingly, *pSMR7::GUS* expression could be observed in the columella and in the vascular tissue, in a similar pattern to *YAK1-GUS*$^{LE}$ grown on AZD-8055 (Fig. 3G). Together, these data suggest that SMRs simultaneously control cells in dividing and differentiated zones of the root depending on relative TOR and YAK1 activities.

Next, we investigated the expression of SMRs in *yak1* mutants and in *YAK1-GUS*$^{OE}$ by RT-qPCR, to confirm our *pSMR:GUS* findings. *SMR4*, *SMR5* and *SMR7* transcripts strongly accumulated when the WT was treated with AZD-8055 (Fig. 5B). There was no accumulation of these transcripts in AZD-8055-treated *yak1-4* and *yak1-7* mutants (Fig. 5B, Fig. S14), indicating that TOR inhibition induces transcription of *SMR4*, *SMR5* and *SMR7* through YAK1. Reciprocally, we observed stronger induction of these three SMR genes when *YAK-GUS*$^{OE}$ was challenged with a low dose of AZD8055 (0.4 µM instead of 1 µM) (Fig. 5C). Together with the strong decrease in MZ size in 0.4 µM AZD8055-treated *YAK-GUS*$^{OE}$ roots (Fig. 3E,F), these results further reinforce the evidence that YAK1 mediates *SMR* induction in response to TOR inhibition.

### YAK1 induces expression of *SMR4* upon TOR inhibition before morphological changes in MZ size occur

In order to determine whether induction of SMRs is associated with early morphological changes in the root, we first analyzed the kinetics of AZD-8055-dependent changes along the root (Fig. 6A). The size of the MZ, EZ and division zone (marked by CYCB1;1-GUS) decreased simultaneously and in the same proportion between 5 and 7 h after transfer onto AZD-8055 (Fig. 6A). This demonstrates that TOR inhibition rapidly lowers the number of dividing and elongating cells in the root. To compare the evolution of cell division with the evolution of *SMR4* expression, we crossed *pSMR4::GUS* and *yak1-1* lines and followed the kinetics of *pSMR4::GUS* expression in WT and *yak1-1* backgrounds (Fig. 6B, Fig. S15). On DMSO, the developmental expression of *pSMR4::GUS* in the *yak1-1* mutant was similar to that of the WT at most time points. This is consistent with the morphology of *yak1* mutants, which is similar to the WT when TOR is not inhibited (Fig. 3). Additionally, the time course on DMSO showed that in both WT and *yak1-1*, TZ/EZ-restricted GUS expression was observed until 7 h, developing into a widespread expression pattern by 24 h before changing again to a strong TZ-restricted expression pattern at 48 h (Fig. 6B). This shows that the dynamics of *SMR4* expression is similarly connected to development in both WT and *yak1-1*. However, GUS expression at 24 h was lower in *yak1-1* (Fig. 6B), indicating that there is constitutive impairment of *SMR4* transcription. This result is consistent with the pINDY-triggered loss of *pSMR4-GUS* expression (Fig. 5) and increase in proliferative cyclins and CCS52A1-GUS (Fig. 4) that we observed in the WT. This again suggests that a certain level of YAK1 activity is present even without TOR inhibitor. In the presence of AZD-8055, the WT expression of *pSMR4::GUS* was more restricted to the MZ/TZ in the first 3 h after transfer, becoming slightly patchy at 5 h before expanding towards the QC at 7 h and to the whole root after 24 h (Fig. 6B). This illustrates the precocious effect of TOR inhibition on *SMR4* expression before any change in MZ size or root growth (Fig. 6A). The WT GUS staining intensity strongly increased between 7 and 24 h on AZD-8055 and then remained high and stable, consistent with the severe slow-down of cell proliferation. Meanwhile, the expression of *pSMR4::GUS* in *yak1-1* was hardly affected by treatment with AZD-8055 up to 24 h, and then clearly decreased at 48 h (Fig. 6B). This shows that YAK1 is required for the proper timing and location of transcriptional regulation of *SMR4* following TOR inhibition. YAK1 ensures the early restriction of *SMR4* expression to the MZ during the first hours of TOR inhibition, then its expansion towards the QC, and finally its strong transcriptional upregulation along the root. This also suggests that the MZ is the first 'checkpoint zone' to be activated to slowdown growth processes at the whole root level. Interestingly, at 48 h after transfer onto AZD-8055, *pSMR4::GUS* expression was almost lost in *yak1-1* (Fig. 6B), reminiscent of the loss of *SMR4* expression observed in WT treated with AZD-8055 and pINDY (Fig. 5A). This shows that YAK1 is required for maintaining *SMR4* expression under TOR inhibition. However, the loss of *SMR4* expression in WT on pINDY alone (Fig. 5A) was not observed in the *yak1-1* mutant at 48 h (Fig. 5B, Fig. 6B). This difference could be explained by different feedback regulation in the knockout of *YAK1* and in pINDY-treated WT. Nevertheless, this kinetic analysis indicates that AZD-8055- and YAK1-dependent changes in *SMR4* expression first occur in the MZ and before morphological changes in the MZ. Therefore, in response to TOR inhibition, modification of *SMR* expression in the meristem could play an early role in triggering the morphological changes that occur later on.

## DISCUSSION

Deciphering a signaling pathway and understanding the role of its components is a huge task that requires several approaches, including gene expression analysis, the study of genetic interactions, and biochemical demonstration of molecular modifications and interactions between components. Pharmacogenetics facilitates the discovery of new components in signaling pathways and the characterization of their physiological role (Xie et al., 2005), especially when mutants are not viable, such as for TOR in *Arabidopsis* (Li et al., 2015; Menand et al., 2002; Montane and Menand, 2013). The development of ATP-competitive kinase inhibitors for medical research, such as AZD-8055 (Chresta et al., 2010), has allowed us to screen for plants resistant to TOR inhibition and isolate three allelic EMS mutants of the DYRK1A/YAK1 kinase.

We have shown that our EMS mutants, *yak1* T-DNA mutants and WT plants treated with the DYRK1A inhibitors INDY and pINDY are similarly resistant to TOR inhibition and that YAK1 overexpressors are reciprocally hypersensitive. Furthermore, YAK1-dependent root growth phenotypes are conditional on TOR inhibition. These data indicate that YAK1 is a repressor of growth that acts downstream of TOR, and represents a new TOR signaling axis in *Arabidopsis* (Figs 1 and 2). Deciphering the mechanism by which active TOR represses YAK1 will require further investigation but knowledge from the animal ortholog DYRK1A indicates that these kinases can be regulated at different levels, including phosphorylation, interaction with regulatory proteins and nuclear translocation (Becker and Sippl, 2011). Our study shows that YAK1 regulates growth by downsizing the meristem and concomitantly promoting differentiation, especially in the stele (Fig. 3). TOR- and YAK1-translational GUS fusions allowed us to show that even

Development (2019) 146, dev171298. doi:10.1242/dev.171298

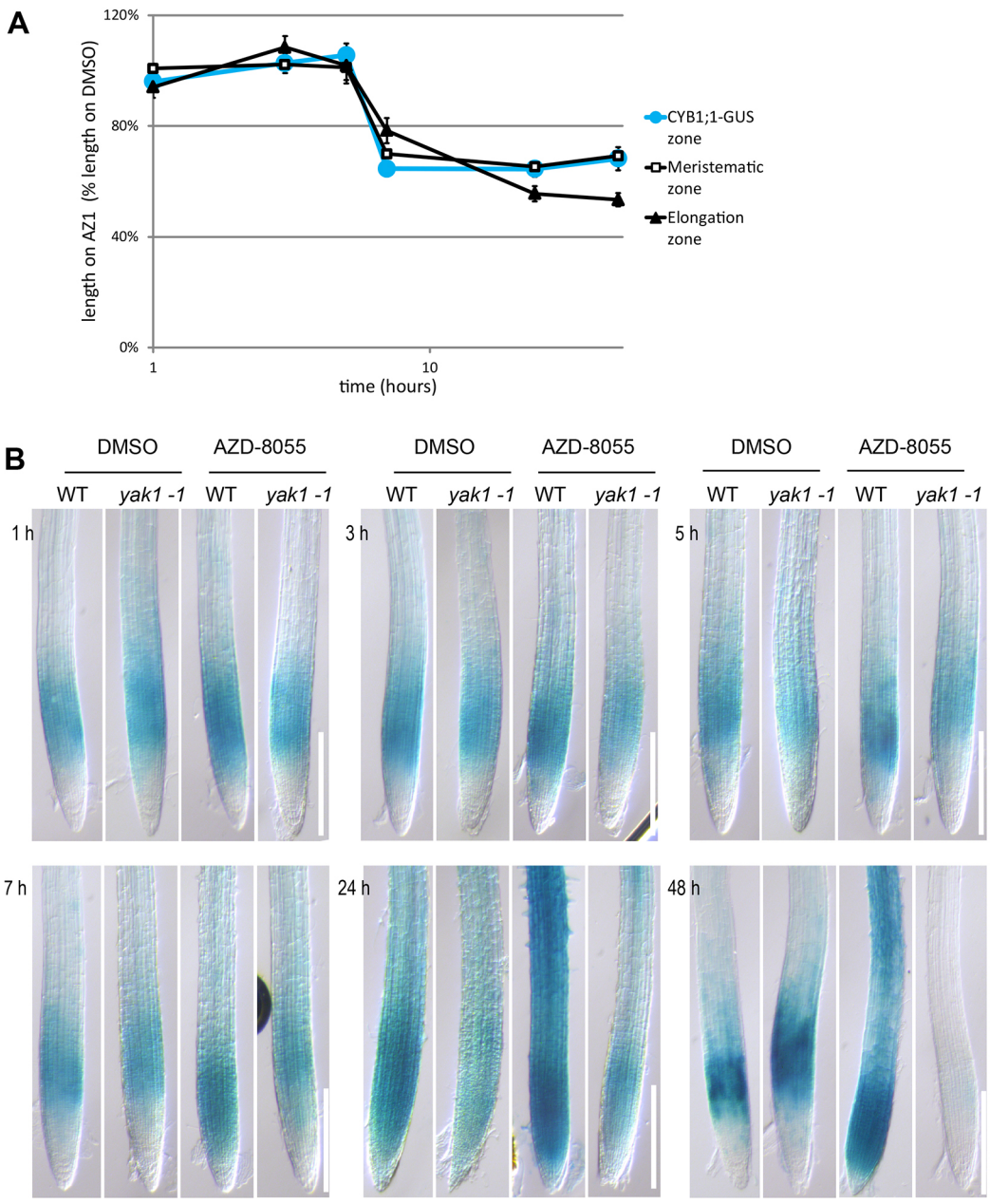


**Fig. 6. Root zone size and spatiotemporal changes of *pSMR4::GUS* expression in WT and *yak1* mutant.** (A) Size of MZ, EZ and division zone (corresponding to the *CYCB1.1-GUS* expression zone) were measured within 48 h after transfer onto DMSO or 1 µM AZD-8055. Standard deviation is shown (*n*=11-20). (B) Time course of *SMR4* expression in root tips of WT Col-0 and of a *yak1-1* line carrying *pSMR4::GUS*, within 48 h of transfer onto DMSO or AZD-8055. Scale bars: 250 µm. A set of images for each condition is provided in Fig. S15.

though YAK1 is expressed across a larger area than TOR in the root, both proteins are co-expressed in the meristem, regardless of the extent of TOR inhibition (Fig. 3G). The YAK1 inhibitor pINDY helped to show that under TOR inhibition YAK1 mainly restrains the root tip expression pattern of CYCs involved in proliferation and formative divisions while inducing the transcription of *SMR4*, *SMR5* and *SMR7* in the whole root (Figs 4 and 5). In addition, SMRs were not induced in response to TOR inhibition in *yak1* mutants and reciprocally they were over-induced by TOR inhibition in the YAK1 overexpressor (Fig. 5B,C, Fig. 6, Fig. S14). As CYCs activate and SMRs repress CDKs (Komaki and Sugimoto, 2012), the opposite expression observed for CYCs and SMRs under TOR inhibition and under YAK1 inhibition indicates that YAK1 activation might contribute to reduction of CDK activity. Most SMRs, including SMR4, SMR5 and SMR7 can functionally complement the *sim* mutant (Kumar et al., 2015), suggesting that they have similar biochemical activity, and that the different isoforms function at specific developmental stages, in certain cell types, or in response to stresses (Hamdoun et al., 2016; Kumar et al., 2015; Yi et al., 2014). Our data show that when TOR is inhibited, *SMR4*, *SMR5* and *SMR7* transcription is simultaneously activated in different parts of the root, namely the QC, initials, columella and vascular tissues for *SMR7*, the division zone for *SMR5*, and the whole root including the meristem and the elongation zone for *SMR4* (Figs 5 and 6). Notably, *SMR4* expression is first induced in a YAK1-dependent manner in the root tip by TOR inhibition, and this occurs earlier than the widespread induction of *SMR4* expression at the whole root level, or the appearance of morphological changes in

Development (2019) 146, dev171298. doi:10.1242/dev.171298

the meristem (Fig. 6). This strongly suggests that TOR inhibition induces a signal that initiates in the MZ and then leads to the upregulation of CDK inhibitors at the whole root level. YAK1 is required for the propagation of this signal. This also supports the hypothesis that SMR-CDK signaling in the root tip plays an important role upstream of morphological changes. Our model is that active TOR represses the growth repressor YAK1 in the MZ. Inactivation of TOR leads to swift YAK1 activation and SMR induction, resulting in the precocious transition from proliferation to differentiation and a swift reduction in MZ size and therefore whole root growth capacity (Fig. 7).

The wider expression pattern of YAK1 compared with TOR suggests that YAK1 may have a role in early steps of differentiation that is independent of TOR (Fig. 3G). This is supported by our observations that pINDY alone slightly increases CYC expression and decreases SMR expression (Figs 4 and 5), and that *SMR4* expression is impaired in the *yak1* mutant at 24 h (Fig. 6). However, this TOR-independent effect is likely to be subtle as no growth defects were observed (Fig. 3) but might reveal a decrease or an absence of YAK1 repression when TOR expression is respectively decreased above the MZ or absent in the columella and the root cap. It is also important to note that *yak1* mutations restore 40-50% of root growth and meristem size under TOR inhibition (Figs 1 and 3). This shows that YAK1 is involved to a large extent in the regulation of growth coordinated by TOR, but also indicates that other regulators of proliferation might act in parallel with YAK1 and downstream of TOR. For instance, *in vitro* assays show that TOR can directly phosphorylate the S phase-specific E2FA transcription factor and the ribosomal protein S6 kinase acting on cell division and protein synthesis (Dobrenel et al., 2016; Xiong et al., 2013; Xiong and Sheen, 2012). However, the contribution of these TOR targets to cell division and meristem size modulation are still not clear and further work is required to determine the specific involvement of these or other regulators in the control of growth by TOR and their crosstalk with YAK1 *in planta*. It could also be interesting to study the contribution of each SMR and of other potential regulators in growth regulation downstream of YAK1. For example, the $Ca^{2+}$ membrane proteins ANNEXIN 1 and 2, which are involved in root growth and phosphorylation of which is altered in the *yak1-1* mutant, could also contribute to YAK1-dependent growth control under stress conditions (Kim et al., 2015; Wang et al., 2018a).

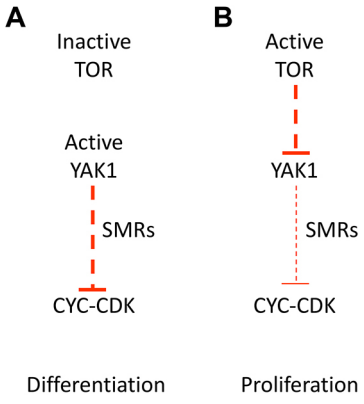


**Fig. 7. Model of the control of meristem activity by the TOR-YAK1 axis.** (A) Under TOR inhibition, active YAK1 induces accumulation of SMRs, which slows cell proliferation and favors early elongation and differentiation leading to repression of root growth. (B) On standard growth medium, active TOR directly or indirectly represses YAK1 to promote maximal meristem activity and size. TOR-dependent regulators other than YAK1 are not included (see Discussion).

YAK1 was first identified in budding yeast because loss of YAK1 function suppresses the cell cycle arrest of a strain lacking catalytic subunits of the cAMP-dependent protein kinase PKA (Garrett and Broach, 1989). The yeast *YAK1* loss-of-function mutant is resistant to rapamycin and it was proposed that yeast TOR might regulate ribosome biogenesis via PKA-dependent repression of YAK1 (Martin et al., 2004). However, these findings should be taken cautiously because a conflicting report proposed that the TOR and PKA signaling pathways act in parallel to promote yeast growth (Ramachandran and Herman, 2011). The situation appears to be different in plants as no PKA ortholog is found in *Arabidopsis* (Wang et al., 2003). In any case, in addition to being a repressor of proliferation in yeast, YAK1 is also required for pseudohyphal growth, hyphal growth, and development of the fruiting body in *Saccharomyces cerevisiae* (Zhang et al., 2001), *Candida albicans* (Goyard et al., 2008) and *Dictyostelium discoideum*, respectively, indicating that YAK1 is an activator of differentiation in these organisms (Souza et al., 1998). In humans, intensive investigation indicates that an additional copy of the *DYRK1A* gene is responsible for some of the neuropathological traits in Down syndrome. In mouse, a modest increase of endogenous DYRK1A protein lengthens the G1 phase of embryonic cortical stem cells, and leads to a deficit in cortical projection neurons (Najas et al., 2015). Overexpression of DYRK1A inhibits proliferation of tumor cell lines from different tissues (Litovchick et al., 2011) whereas DYRK1A inhibitors such as INDY are mitogenic (Wang et al., 2015), indicating that DYRK1A is a general repressor of mammalian cell proliferation. Reciprocally, loss of function of *Drosophila* Minibrain/DYRK1A leads to over-proliferation of neuronal precursors that fail to differentiate and die by apoptosis, resulting in a small brain (Shaikh et al., 2016). At the molecular level, DYRK1A acts via cell cycle-associated proteins (Fernández-Martinez et al., 2015). Mammalian DYRK1A induces transcriptional upregulation and phosphorylation of the CDK inhibitor $p27^{Kip1}$ (CDKN1B) and mediates the phosphorylation of cyclins D1 and D3, leading respectively to $p27^{Kip1}$ stabilization and cyclin degradation (Hammerle et al., 2011; Soppa et al., 2014; Thompson et al., 2015). In a similar trend, genetic studies suggest that YAK1 enhances the APC-mediated ubiquitylation and destruction of cyclin B in yeast (Jaspersen et al., 1998). Therefore, in comparison with previous work on animals and yeast, our data support a conserved function for DYRK1A/YAK1 as a repressor of proliferation via transcriptional and/or post-translational control of cell cycle regulators, and an activator of differentiation in eukaryotes. However, even though these functions are conserved, particular aspects of plant growth, such as their iterative development, might explain why YAK1 loss of function or overexpression results in distinct phenotypes in animals and plants. Understanding how the detailed mechanisms underlying YAK1 function in plants have been conserved, as well as the relationship between TOR and DYRK1A/YAK1 will require further investigation. Hence, no connection between animal DYRK1A and TOR has so far been described but our work presented here opens up the possibility that there is a conserved link between TOR and DYRK1A/YAK1 in animals.

Complex hormone crosstalk regulates plant growth under various environmental conditions. In each root zone, different hormone networks interact with one another through cell- and tissue-specific titrations that coordinately control quiescence, cell proliferation, and differentiation (Pacifici et al., 2015; Takatsuka and Umeda, 2014). Indeed, TOR is essential for meristem development and its activity has already been shown to be related to auxin, brassinosteroid and

Development (2019) 146, dev171298. doi:10.1242/dev.171298

gibberellin, which promote cell proliferation via repression of CDK inhibitors in the MZ, and also to ABA, which inhibits cell division in response to stress (Li et al., 2017; Montane and Menand, 2013; Schepetilnikov et al., 2017; Wang et al., 2018b; Xiong et al., 2013; Zhang et al., 2016). YAK1 has been the subject of less work in plants, but primary root elongation of *yak1-1* mutant is partially resistant to exogenous ABA treatment (Kim et al., 2016), whereas mutants in members of the TOR complex are hypersensitive to ABA (Kravchenko et al., 2015). Furthermore, ABA triggers TOR inhibition through SnRK2-mediated phosphorylation of RAPTOR (Wang et al., 2018b). Together with our data, this suggests that ABA might repress growth via TOR inhibition-dependent activation of YAK1. Therefore, the TOR pathway is likely to act as a central integrator of the hormone crosstalk regulating meristem activity (Barrada et al., 2015) together with the control of cell cycle effectors as we have shown in this work. Interestingly, YAK1 interacts with circadian clock components and is required for the optimization of photomorphogenesis and reproductive development (Huang et al., 2017), underscoring the role of YAK1 in shoot and flower development, two processes also regulated by TOR (Bakshi et al., 2017; Deprost et al., 2007; Moreau et al., 2012; Ren et al., 2012). At the metabolic level, TOR and YAK1 have antagonist roles in the regulation of triacylglycerol accumulation in algae (Imamura et al., 2016; Kajikawa et al., 2015; Prioretti et al., 2017). Altogether, these diverse phenotypes might have in common similar TOR activity-dependent early molecular events that could ultimately change cell fate depending on environmental conditions. Here, we demonstrate that the TOR-YAK1 axis plays a crucial role in regulating root meristem activity, and in the future it will be fascinating to reveal the full extent of TOR-YAK1 signaling.

## MATERIALS AND METHODS

### Plant material

The *Arabidopsis* WT used for the mutagenesis was the Columbia (Col-0) line carrying the null allele *erecta-105*, named Col$^{er105}$ (Balzergue et al., 2017). The latter does not affect sensitivity to AZD-8055 (Fig. S16). The three *YAK1* EMS mutants isolated in our screen were called *yak1-4*, *yak1-5* and *yak1-6*. Both *yak1-4* and *yak1-6* were backcrossed two times to Col$^{er105}$ before being used in all experiments. *yak1-5* had a fertility defect that made crossings very difficult. However, we managed to cross this mutant with Col-3, which allowed us to study the segregation of the *yak1-5* resistance phenotype on AZD-8055. We chose *yak1-1* (SAIL_31_C10) T-DNA insertion line because *YAK1* knockout was already confirmed by RT-PCR (Kim et al., 2015). Isogenic Col-3 was isolated and used as the control line for this mutant. In order to have another T-DNA mutant in the Col-0 background, we selected line SALK_208347C (*yak1-7*), which was confirmed to be a null mutant by RT-PCR (Fig. S17). *pCYCB1;1::CYCB1;1-GUS* (named here *CYCB1;1-GUS*) and *TOR::GUS* (*TOR/tor-1*) lines were described previously (Colon-Carmona et al., 1999; Menand et al., 2002). *pCYCA/B::CYC-GUS* translational fusion lines (named here *CYCA/B-GUS*) (Bulankova et al., 2013), *yak1-1* and *yak1-7* were acquired from the Nottingham Arabidopsis Stock Centre (NASC). The *BP12-2* (*p35S:FKBP12-GFP*) line was provided by M. Ren (Ren et al., 2012). The *pCYCD::GUS-GFP* transcriptional fusions (named here *pCYCD::GUS*) were received from J. A. H. Murray and J. Kilby (Forzani et al., 2014; Sozzani et al., 2010). The *pCCS52A1::GUS* line was obtained from N. Takahashi and E. Kondorosi (Vanstraelen et al., 2009). *pSIM/SMR::GFP-GUS* reporter lines (named here *pSIM/SMR::GUS*) were from L. De Veylder (Yi et al., 2014).

### *In vitro* plant growth and drug treatment

Plants were grown on solid medium prepared as described previously (Montane and Menand, 2013) with addition of 2.5 mM 2-(N-morpholino) ethanesulfonic acid (MES) to buffer the pH (5.5). All drugs were dissolved in pure 0.2 µm filter-sterilized DMSO. The final concentration of DMSO in mock plates as well as drug-containing plates was 0.1%, which does not affect root growth (Montane and Menand, 2013). Seeds were surface-sterilized and germinated on solid medium for 3 days before transferring plantlets to drug-containing medium. Petri dishes containing 25 ml of medium were used and placed vertically to allow the roots to grow on the surface of the medium. A photoperiod of 16 h at 23°C (80 µmol photons $m^{-2}$ $s^{-1}$) was followed by 8 h of dark at 18°C. AZD-8055 and WYE-132 were purchased from Chemdea (Ridgewood, USA), Rapamycin was purchased from LC Labs (Woburn, USA), INDY and pINDY were supplied by Glixx lab (Hopkinton, USA).

### Root growth measurements

The position of the tip of each primary root was labeled every day on the back of the Petri dish. Five days after transfer to the new medium containing drug(s) or DMSO, Petri dishes were scanned (EPSON Perfection 1250, EPSON TWAIN5 software) and primary root growth was measured using ImageJ software.

### Mutagenesis and mutant screen

The screen for AZD-8055 resistant mutants was performed with an EMS mutants library previously described (Balzergue et al., 2017). Briefly, about $8\times10^4$ Col$^{er105}$ seeds were mutagenized and sown on soil and the M2 generation was collected in 156 pools of 400-500 M1 plants each. About 2500 seeds from 44 of these 156 pools were sown on square plates (12×12 cm) containing 1 µM AZD-8055 (plates contained two horizontal lines of about 1250 seeds each). After 48 h at 4°C, plates were placed vertically in the growth chamber. Seven days later, plates were screened for seedlings with a longer primary root compared with the majority of neighboring roots, and putative resistant mutants were transferred for 5 days onto fresh plates containing 1 µM AZD-8055. Mutants that still showed the phenotype were transplanted into soil. A secondary screen was performed by comparing the M3 progeny root length with the WT on 1 µM AZD-8055 and DMSO. DNA samples of seven clearly resistant mutants from different pools were sequenced.

### Next-generation DNA sequencing and single nucleotide polymorphism identification

Genomic DNA was extracted from the same plants that were used for the backcrosses, using the NucleoSpin Plant II Maxi kit (Machery-Nagel) with PL1 buffer and polyvinylpolypyrrolidone (PVPP, at half the plant tissue weight). DNA-seq library preparation and whole genome sequencing (Illumina Highseq2000, 125 pb) were carried out by the TGAC/Earlham Institute NGS platform (Norwich, UK). A list of single nucleotide polymorphism (SNPs) was generated through comparison with the reference genome of *A. thaliana* TAIR 10 (Col-0) using the mutdetect pipeline (Girard et al., 2014). SNPs shared with the WT (Col$^{er105}$) were eliminated by the FileMatch program. Both mutdetect and FileMatch were developed by the Institut Jean-Pierre Bourgin (IJPB) bioinformatics team (INRA, AgroParisTech, CNRS, Université Paris-Saclay, Versailles, France). SNP lists were filtered for homozygous, non-synonymous or splicing site mutations. The SNP lists of the seven mutants were compared with one another in order to find common mutated genes.

### Genotyping of mutants

We used cleaved amplification polymorphic sequences (CAPS) for EMS mutant genotyping. For each mutant, we designed specific primers in order to amplify the mutated *YAK1* sequence (Table S4). PCR was performed using Taq'Ozyme Purple Mix2 (Takara Bio) and fragments were digested with restriction enzymes (NEB) targeting the mutated or WT locus (Table S4) in order to differentiate WT from mutant PCR products by gel electrophoresis. *YAK1* T-DNA lines were genotyped with two genomic primers flanking the T-DNA insertion and a T-DNA LB primer (Table S4).

### Cloning and plant transformation

The *pYAK1::YAK1-GUS* construct was made by amplifying the *YAK1* genomic sequence from the promoter to the end of the coding region (see Table S4 for primers) and cloning the resulting PCR product, in-frame with the *GUS* coding sequence, into the pBI101 plasmid using the *Sal*I/*Sma*I sites

Development (2019) 146, dev171298. doi:10.1242/dev.171298

(Fig. S7A). *pYAK1::YAK1-GUS* was transformed into *Arabidopsis* by floral dip and transgenic plants were selected on kanamycin plates (50 µM). The T3 generation was screened for homozygous lines carrying different levels of GUS expression (Fig. S9B).

### GUS histochemical staining

Plants were incubated in GUS staining solution as described previously (Montane and Menand, 2013) for 4 h (*pYAK1::YAK1-GUS*, *TOR::GUS*, *pCYCD3;3::GUS*, *pCCS52A1::GUS*, *pSIM/SMR::GUS*) or 24 h (all remaining lines). Plants were then washed with 10 mM sodium phosphate buffer and stored in a chloral hydrate solution (100 g chloral hydrate, 30 ml water and 5 ml glycerin) at 4°C.

### Microscopy

Images showing the differentiated zone containing root hairs were taken directly from the Petri dish using a Stereo Discovery V12 stereomicroscope (Zeiss). For GUS expression pattern observations, roots were mounted in chloral hydrate and observed with the stereomicroscope. For *pYAK1::YAK1-GUS* and *TOR::GUS* expression pattern and for meristem observations, roots were mounted in chloral hydrate and observed using an Axio imager M2 microscope (Zeiss) with a DIC illumination system. DIC images were assembled using the photomerge tool of Adobe Photoshop, in order to reconstitute high magnification pictures of primary root meristems. All images are representative of at least six plants. Meristem length, cell surface area and epidermal cell length were measured with ImageJ. The size of the MZ, corresponding to the distance between the QC and the first elongated cortical cell, was measured as described previously (Perilli and Sabatini, 2010). Epidermal cell length measurements were obtained by taking the distance between two consecutive root hairs of the same cell file.

### RNA isolation, qRT-PCR and RT-PCR

For qRT-PCR, seeds were sown in line on sterile nylon mesh (1.5 cm×6.5, 100 µm), incubated for 2 days at 4°C and grown for 7 days on drug-free medium before transfer onto drug-containing medium with the nylon mesh. After 48 h, total RNA was extracted from whole roots using TriReagent (Sigma-Aldrich), quality was confirmed by gel electrophoresis, and genomic DNA removed by treatment with DNase I (Thermo Scientific). cDNA was then synthesized from 500 ng RNA using a Primescript RT Reagent Kit (Takara Bio) with random hexamer and oligo(dT) primers. qRT-PCR was performed on 1 µl of half-diluted cDNA in 15 µl reactions using SYBR Premix Ex-Taq II reagent (Takara Bio) in a Bio-Rad CFX96 real-time system (see Table S4 for primers). Relative quantification of gene expression adjusted for efficiency was performed using PCR Miner (Zhao and Fernald, 2005). *ACTIN 2* and *PROFILIN 1* were used as reference genes. Their stability values were within the advised limits (M<0.5 and Cv<0.25) (Vandesompele et al., 2002). For *YAK1* knockout confirmation, RNA was isolated from inflorescences and treated as previously stated. RT-PCRs were performed on 1 µl cDNA using Taq'Ozyme Purple Mix2 (see Table S4 for primers).

### Statistical tests

Results are presented as mean±s.e.m. Statistical analyses were performed using R, Excel and XLSTAT. Sample size was not predetermined using statistical methods, but took into account the variability of the traits measured, assessed by the standard deviation. The two-tailed Student's *t*-test was used to compare WT samples with mutant samples. One-way or two-way ANOVA were used to compare multiple sample means, with post-hoc Dunnett test. Mean values that do not share the same letter are significantly different. The results for statistical significance tests are included in the legend of each figure; *n* values represent the number of biological replicates or the number of seedlings, meristems per condition.

#### Acknowledgements

We acknowledge M. Ren, J. A. H. Murray, J. Kilby, N. Takahashi, E. Kondorosi, L. De Veylder and the NASC for providing seeds. We thank F. Granier for helping us with NGS sequence analysis, P. De Sepulveda for suggesting the use of metaSNP and C. Godon for sharing *in vitro* growth protocols. The microscopy was performed in the IBDML imaging facility of Aix-Marseille University. We thank B. Field for helping with qRT-PCR analysis and for critical reading of the manuscript.

#### Competing interests

The authors declare no competing or financial interests.

#### Author contributions

Conceptualization: A.B., M.-H.M., B.M.; Methodology: A.B., R.M., M.-H.M., B.M.; Software: R.M.; Validation: A.B., M.-H.M., B.M.; Formal analysis: A.B., M.-H.M., B.M.; Investigation: A.B., M.D., M.-H.M., B.M.; Resources: T.D.; Data curation: A.B., M.-H.M., B.M.; Writing - original draft: A.B., M.-H.M., B.M.; Writing - review & editing: A.B., T.D., R.M., C.R., M.-H.M., B.M.; Visualization: A.B., M.-H.M., B.M.; Supervision: M.-H.M., B.M.; Project administration: C.R., B.M.; Funding acquisition: C.R., M.-H.M., B.M.

#### Funding

This work was funded by the French Agence Nationale de la Recherche (ANR-14-CE19-0007).

#### Supplementary information

Supplementary information available online at
http://dev.biologists.org/lookup/doi/10.1242/dev.171298.supplemental

#### References

**Ahn, C. S., Han, J.-A., Lee, H.-S., Lee, S. and Pai, H.-S.** (2011). The PP2A regulatory subunit Tap46, a component of the TOR signaling pathway, modulates growth and metabolism in plants. *Plant Cell* **23**, 185-209.

**Ahn, C. S., Ahn, H.-K. and Pai, H.-S.** (2015). Overexpression of the PP2A regulatory subunit Tap46 leads to enhanced plant growth through stimulation of the TOR signalling pathway. *J. Exp. Bot.* **66**, 827-840.

**Aranda, S., Laguna, A. and De la Luna, S.** (2011). DYRK family of protein kinases: evolutionary relationships, biochemical properties, and functional roles. *FASEB J.*. **25**, 449-462.

**Bakshi, A., Moin, M., Kumar, M. U., Reddy, A. B. M., Ren, M., Datla, R., Siddiq, E. A. and Kirti, P. B.** (2017). Ectopic expression of Arabidopsis Target of Rapamycin (AtTOR) improves water-use efficiency and yield potential in rice. *Sci. Rep.* **7**, 42835.

**Balzergue, C., Dartevelle, T., Godon, C., Laugier, E., Meisrimler, C., Teulon, J.-M., Creff, A., Bissler, M., Brouchoud, C., Hagège, A. et al.** (2017). Low phosphate activates STOP1-ALMT1 to rapidly inhibit root cell elongation. *Nat. Commun.* **8**, 15300.

**Barrada, A., Montané, M.-H., Robaglia, C. and Menand, B.** (2015). Spatial regulation of root growth: placing the plant TOR pathway in a developmental perspective. *Int. J. Mol. Sci.* **16**, 19671-19697.

**Becker, W. and Sippl, W.** (2011). Activation, regulation, and inhibition of DYRK1A. *FEBS J.* **278**, 246-256.

**Beemster, G. T. and Baskin, T. I.** (1998). Analysis of cell division and elongation underlying the developmental acceleration of root growth in Arabidopsis thaliana. *Plant Physiol.* **116**, 1515-1526.

**Ben-Sahra, I. and Manning, B. D.** (2017). mTORC1 signaling and the metabolic control of cell growth. *Curr. Opin. Cell Biol.* **45**, 72-82.

**Boudolf, V., Lammens, T., Boruc, J., Van Leene, J., Van Den Daele, H., Maes, S., Van Isterdael, G., Russinova, E., Kondorosi, E., Witters, E. et al.** (2009). CDKB1;1 forms a functional complex with CYCA2;3 to suppress endocycle onset. *Plant Physiol.* **150**, 1482-1493.

**Breuer, C., Braidwood, L. and Sugimoto, K.** (2014). Endocycling in the path of plant development. *Curr. Opin. Plant Biol.* **17**, 78-85.

**Bulankova, P., Akimcheva, S., Fellner, N. and Riha, K.** (2013). Identification of Arabidopsis meiotic cyclins reveals functional diversification among plant cyclin genes. *PLoS Genet.* **9**, e1003508.

**Caldana, C., Li, Y., Leisse, A., Zhang, Y., Bartholomaeus, L., Fernie, A. R., Willmitzer, L. and Giavalisco, P.** (2013). Systemic analysis of inducible target of rapamycin mutants reveal a general metabolic switch controlling growth in Arabidopsis thaliana. *Plant J.* **73**, 897-909.

**Capriotti, E., Altman, R. B. and Bromberg, Y.** (2013). Collective judgment predicts disease-associated single nucleotide variants. *BMC Genomics* **14** Suppl. 3, S2.

**Chresta, C. M., Davies, B. R., Hickson, I., Harding, T., Cosulich, S., Critchlow, S. E., Vincent, J. P., Ellston, R., Jones, D., Sini, P. et al.** (2010). AZD8055 is a potent, selective, and orally bioavailable ATP-competitive mammalian target of rapamycin kinase inhibitor with in vitro and in vivo antitumor activity. *Cancer Res.* **70**, 288-298.

**Churchman, M. L., Brown, M. L., Kato, N., Kirik, V., Hulskamp, M., Inze, D., De Veylder, L., Walker, J. D., Zheng, Z., Oppenheimer, D. G. et al.** (2006). SIAMESE, a plant-specific cell cycle regulator, controls endoreplication onset in Arabidopsis thaliana. *Plant Cell* **18**, 3145-3157.

**Collins, C., Maruthi, N. M. and Jahn, C. E.** (2015). CYCD3 D-type cyclins regulate cambial cell proliferation and secondary growth in Arabidopsis. *J. Exp. Bot.* **66**, 4595-4606.

**Colon-Carmona, A., You, R., Haimovitch-Gal, T. and Doerner, P.** (1999). Technical advance: spatio-temporal analysis of mitotic activity with a labile cyclin-GUS fusion protein. *Plant J.* **20**, 503-508.

**De Veylder, L., Larkin, J. C. and Schnittger, A.** (2011). Molecular control and function of endoreplication in development and physiology. *Trends Plant Sci.* **16**, 624-634.
**Deprost, D., Yao, L., Sormani, R., Moreau, M., Leterreux, G., Nicolaï, M., Bedu, M., Robaglia, C. and Meyer, C.** (2007). The Arabidopsis TOR kinase links plant growth, yield, stress resistance and mRNA translation. *EMBO Rep.* **8**, 864-870.
**Dobrenel, T., Mancera-Martinez, E., Forzani, C., Azzopardi, M., Davanture, M., Moreau, M., Schepetilnikov, M., Chicher, J., Langella, O., Zivy, M. et al.** (2016). The Arabidopsis TOR kinase specifically regulates the expression of nuclear genes coding for plastidic ribosomal proteins and the phosphorylation of the cytosolic ribosomal protein S6. *Front. Plant Sci.* **7**, 1611.
**Dong, P., Xiong, F., Que, Y., Wang, K., Yu, L., Li, Z. and Ren, M.** (2015). Expression profiling and functional analysis reveals that TOR is a key player in regulating photosynthesis and phytohormone signaling pathways in Arabidopsis. *Front. Plant Sci.* **6**, 677.
**Fernández-Martinez, P., Zahonero, C. and Sanchez-Gomez, P.** (2015). DYRK1A: the double-edged kinase as a protagonist in cell growth and tumorigenesis. *Mol. Cell. Oncol.* **2**, e970048.
**Forzani, C., Aichinger, E., Sornay, E., Willemsen, V., Laux, T., Dewitte, W. and Murray, J. A. H.** (2014). WOX5 suppresses CYCLIN D activity to establish quiescence at the center of the root stem cell niche. *Curr. Biol.* **24**, 1939-1944.
**Garrett, S. and Broach, J.** (1989). Loss of Ras activity in Saccharomyces cerevisiae is suppressed by disruptions of a new kinase gene, YAKI, whose product may act downstream of the cAMP-dependent protein kinase. *Genes Dev.*. **3**, 1336-1348.
**Girard, C., Crismani, W., Froger, N., Mazel, J., Lemhemdi, A., Horlow, C. and Mercier, R.** (2014). FANCM-associated proteins MHF1 and MHF2, but not the other Fanconi anemia factors, limit meiotic crossovers. *Nucleic Acids Res.* **42**, 9087-9095.
**Gonzalez, S. and Rallis, C.** (2017). The TOR signaling pathway in spatial and temporal control of cell size and growth. *Front. Cell Dev. Biol.* **5**, 61.
**Goyard, S., Knechtle, P., Chauvel, M., Mallet, A., Prévost, M.-C., Proux, C., Coppée, J.-Y., Schwarz, P., Dromer, F., Park, H. et al.** (2008). The Yak1 kinase is involved in the initiation and maintenance of hyphal growth in Candida albicans. *Mol. Biol. Cell* **19**, 2251-2266.
**Hamdoun, S., Zhang, C., Gill, M., Kumar, N., Churchman, M., Larkin, J. C., Kwon, A. and Lu, H.** (2016). Differential roles of two homologous cyclin-dependent kinase inhibitor genes in regulating cell cycle and innate immunity in arabidopsis. *Plant Physiol.* **170**, 515-527.
**Hammerle, B., Ulin, E., Guimera, J., Becker, W., Guillemot, F. and Tejedor, F. J.** (2011). Transient expression of Mnb/Dyrk1a couples cell cycle exit and differentiation of neuronal precursors by inducing p27KIP1 expression and suppressing NOTCH signaling. *Development* **138**, 2543-2554.
**Huang, W. Y., Wu, Y. C., Pu, H. Y., Wang, Y., Jang, G. J. and Wu, S. H.** (2017). Plant dual-specificity tyrosine phosphorylation-regulated kinase optimizes light-regulated growth and development in Arabidopsis. *Plant Cell Environ.* **40**, 1735-1747.
**Imai, K. K., Ohashi, Y., Tsuge, T., Yoshizumi, T., Matsui, M., Oka, A. and Aoyama, T.** (2006). The A-type cyclin CYCA2;3 is a key regulator of ploidy levels in Arabidopsis endoreduplication. *Plant Cell* **18**, 382-396.
**Imamura, S., Kawase, Y., Kobayashi, I., Shimojima, M., Ohta, H. and Tanaka, K.** (2016). TOR (target of rapamycin) is a key regulator of triacylglycerol accumulation in microalgae. *Plant. Signal. Behav.* **11**, e1149285.
**Inagaki, S. and Umeda, M.** (2011). Cell-cycle control and plant development. *Int. Rev. Cell Mol. Biol.* **291**, 227-261.
**Jaspersen, S. L., Charles, J. F., Tinker-Kulberg, R. L. and Morgan, D. O.** (1998). A late mitotic regulatory network controlling cyclin destruction in Saccharomyces cerevisiae. *Mol. Biol. Cell* **9**, 2803-2817.
**Kajikawa, M., Sawaragi, Y., Shinkawa, H., Yamano, T., Ando, A., Kato, M., Hirono, M., Sato, N. and Fukuzawa, H.** (2015). Algal dual-specificity tyrosine phosphorylation-regulated kinase, triacylglycerol accumulation regulator1, regulates accumulation of triacylglycerol in nitrogen or sulfur deficiency. *Plant Physiol.*. **168**, 752-764.
**Karpov, P., Raevsky, A., Korablyov, M. and Blume, Y.** (2014). Identification of plant homologues of dual specificity Yak1-related kinases. *Comput. Bio. J.* **2014**, 909268.
**Kim, D., Ntui, V. O., Zhang, N. and Xiong, L.** (2015). Arabidopsis Yak1 protein (AtYak1) is a dual specificity protein kinase. *FEBS Lett.* **589**, 3321-3327.
**Kim, D., Ntui, V. O. and Xiong, L.** (2016). Arabidopsis YAK1 regulates abscisic acid response and drought resistance. *FEBS Lett.* **590**, 2201-2209.
**Komaki, S. and Sugimoto, K.** (2012). Control of the plant cell cycle by developmental and environmental cues. *Plant Cell Physiol.* **53**, 953-964.
**Kravchenko, A., Citerne, S., Jéhanno, I., Bersimbaev, R. I., Veit, B., Meyer, C. and Leprince, A.-S.** (2015). Mutations in the Arabidopsis Lst8 and Raptor genes encoding partners of the TOR complex, or inhibition of TOR activity decrease abscisic acid (ABA) synthesis. *Biochem. Biophys. Res. Commun.* **467**, 992-997.
**Kumar, N., Harashima, H., Kalve, S., Bramsiepe, J., Wang, K., Sizani, B. L., Bertrand, L. L., Johnson, M. C., Faulk, C., Dale, R. et al.** (2015). Functional conservation in the SIAMESE-RELATED family of cyclin-dependent kinase inhibitors in land plants. *Plant Cell* **27**, 3065-3080.
**Leiber, R.-M., John, F., Verhertbruggen, Y., Diet, A., Knox, J. P. and Ringli, C.** (2010). The TOR pathway modulates the structure of cell walls in Arabidopsis. *Plant Cell* **22**, 1898-1908.
**Li, L., Song, Y., Wang, K., Dong, P., Zhang, X., Li, F., Li, Z. and Ren, M.** (2015). TOR-inhibitor insensitive-1 (TRIN1) regulates cotyledons greening in Arabidopsis. *Front. Plant Sci.* **6**, 861.
**Li, X., Cai, W., Liu, Y., Li, H., Fu, L., Liu, Z., Xu, L., Liu, H., Xu, T. and Xiong, Y.** (2017). Differential TOR activation and cell proliferation in Arabidopsis root and shoot apexes. *Proc. Natl. Acad. Sci. USA* **114**, 2765-2770.
**Litovchick, L., Florens, L. A., Swanson, S. K., Washburn, M. P. and DeCaprio, J. A.** (2011). DYRK1A protein kinase promotes quiescence and senescence through DREAM complex assembly. *Genes Dev.* **25**, 801-813.
**Loewith, R. and Hall, M. N.** (2011). Target of rapamycin (TOR) in nutrient signaling and growth control. *Genetics* **189**, 1177-1201.
**Mahfouz, M. M., Kim, S., Delauney, A. J. and Verma, D. P.** (2006). Arabidopsis TARGET OF RAPAMYCIN interacts with RAPTOR, which regulates the activity of S6 kinase in response to osmotic stress signals. *Plant Cell* **18**, 477-490.
**Martin, D. E., Soulard, A. and Hall, M. N.** (2004). TOR regulates ribosomal protein gene expression via PKA and the Forkhead transcription factor FHL1. *Cell* **119**, 969-979.
**Meijer, L., Borgne, A., Mulner, O., Chong, J. P. J., Blow, J. J., Inagaki, N., Inagaki, M., Delcros, J.-G. and Moulinoux, J.-P.** (1997). Biochemical and cellular effects of roscovitine, a potent and selective inhibitor of the cyclin-dependent kinases cdc2, cdk2 and cdk5. *Eur. J. Biochem.* **243**, 527-536.
**Menand, B., Desnos, T., Nussaume, L., Berger, F., Bouchez, D., Meyer, C. and Robaglia, C.** (2002). Expression and disruption of the Arabidopsis TOR (target of rapamycin) gene. *Proc. Natl. Acad. Sci. USA* **99**, 6422-6427.
**Montane, M.-H. and Menand, B.** (2013). ATP-competitive mTOR kinase inhibitors delay plant growth by triggering early differentiation of meristematic cells but no developmental patterning change. *J. Exp. Bot.* **64**, 4361-4374.
**Moreau, M., Azzopardi, M., Clement, G., Dobrenel, T., Marchive, C., Renne, C., Martin-Magniette, M.-L., Taconnat, L., Renou, J.-P., Robaglia, C. et al.** (2012). Mutations in the Arabidopsis homolog of LST8/GbetaL, a partner of the target of Rapamycin kinase, impair plant growth, flowering, and metabolic adaptation to long days. *Plant Cell* **24**, 463-481.
**Najas, S., Arranz, J., Lochhead, P. A., Ashford, A. L., Oxley, D., Delabar, J. M., Cook, S. J., Barallobre, M. J. and Arbonés, M. L.** (2015). DYRK1A-mediated cyclin D1 Degradation in neural stem cells contributes to the neurogenic cortical defects in Down syndrome. *EBioMedicine* **2**, 120-134.
**Odawara, M., Kadowaki, T., Yamamoto, R., Shibasaki, Y., Tobe, K., Accili, D., Bevins, C., Mikami, Y., Matsuura, N., Akanuma, Y. et al.** (1989). Human diabetes associated with a mutation in the tyrosine kinase domain of the insulin receptor. *Science* **245**, 66-68.
**Ogawa, Y., Nonaka, Y., Goto, T., Ohnishi, E., Hiramatsu, T., Kii, I., Yoshida, M., Ikura, T., Onogi, H., Shibuya, H. et al.** (2010). Development of a novel selective inhibitor of the Down syndrome-related kinase Dyrk1A. *Nat. Commun.* **1**, 86.
**Ouibrahim, L., Rubio, A. G., Moretti, A., Montané, M.-H., Menand, B., Meyer, C., Robaglia, C. and Caranta, C.** (2015). Potyviruses differ in their requirement for TOR signalling. *J. Gen. Virol.* **96**, 2898-2903.
**Pacifici, E., Polverari, L. and Sabatini, S.** (2015). Plant hormone cross-talk: the pivot of root growth. *J. Exp. Bot.* **66**, 1113-1121.
**Perilli, S. and Sabatini, S.** (2010). Analysis of root meristem size development. *Methods Mol. Biol.* **655**, 177-187.
**Pfeiffer, A., Janocha, D., Dong, Y., Medzihradszky, A., Schone, S., Daum, G., Suzaki, T., Forner, J., Langenecker, T., Rempel, E. et al.** (2016). Integration of light and metabolic signals for stem cell activation at the shoot apical meristem. *Elife* **5**, e17023.
**Prioretti, L., Avilan, L., Carriere, F., Montane, M. H., Field, B., Gregori, G., Menand, B. and Gontero, B.** (2017). The inhibition of TOR in the model diatom Phaeodactylum tricornutum promotes a get-fat growth regime. *Algal Res.* **26**, 265-274.
**Pu, Y., Luo, X. and Bassham, D. C.** (2017). TOR-dependent and -independent pathways regulate autophagy in arabidopsis thaliana. *Front. Plant Sci.* **8**, 1204.
**Ramachandran, V. and Herman, P. K.** (2011). Antagonistic interactions between the cAMP-dependent protein kinase and Tor signaling pathways modulate cell growth in Saccharomyces cerevisiae. *Genetics* **187**, 441-454.
**Ren, M., Venglat, P., Qiu, S., Feng, L., Cao, Y., Wang, E., Xiang, D., Wang, J., Alexander, D., Chalivendra, S. et al.** (2012). Target of rapamycin signaling regulates metabolism, growth, and life span in Arabidopsis. *Plant Cell* **24**, 4850-4874.
**Salem, M. A., Li, Y., Wiszniewski, A. and Giavalisco, P.** (2017). Regulatory-associated protein of TOR (RAPTOR) alters the hormonal and metabolic composition of Arabidopsis seeds, controlling seed morphology, viability and germination potential. *Plant J.* **92**, 525-545.
**Schepetilnikov, M., Makarian, J., Srour, O., Geldreich, A., Yang, Z., Chicher, J., Hammann, P. and Ryabova, L. A.** (2017). GTPase ROP2 binds and promotes activation of target of rapamycin, TOR, in response to auxin. *EMBO J.* **36**, 886-903.
**Seu, L., Sabbaj, S., Duverger, A., Wagner, F., Anderson, J. C., Davies, E., Wolschendorf, F., Willey, C. D., Saag, M. S., Goepfert, P. et al.** (2015). Stable

phenotypic changes of the host T cells are essential to the long-term stability of latent HIV-1 infection. *J. Virol.* **89**, 6656-6672.

**Shaikh, M. N., Gutierrez-Aviño, F., Colonques, J., Ceron, J., Hammerle, B. and Tejedor, F. J.** (2016). Minibrain drives the Dacapo-dependent cell cycle exit of neurons in the Drosophila brain by promoting asense and prospero expression. *Development* **143**, 3195-3205.

**Soppa, U., Schumacher, J., Florencio Ortiz, V., Pasqualon, T., Tejedor, F. J. and Becker, W.** (2014). The Down syndrome-related protein kinase DYRK1A phosphorylates p27(Kip1) and Cyclin D1 and induces cell cycle exit and neuronal differentiation. *Cell Cycle* **13**, 2084-2100.

**Souza, G. M., Lu, S. and Kuspa, A.** (1998). YakA, a protein kinase required for the transition from growth to development in Dictyostelium. *Development* **125**, 2291-2302.

**Sozzani, R., Cui, H., Moreno-Risueno, M. A., Busch, W., Van Norman, J. M., Vernoux, T., Brady, S. M., Dewitte, W., Murray, J. A. and Benfey, P. N.** (2010). Spatiotemporal regulation of cell-cycle genes by SHORTROOT links patterning and growth. *Nature* **466**, 128-132.

**Sugimoto-Shirasu, K. and Roberts, K.** (2003). 'Big it up': endoreduplication and cell-size control in plants. *Curr. Opin. Plant Biol.* **6**, 544-553.

**Takatsuka, H. and Umeda, M.** (2014). Hormonal control of cell division and elongation along differentiation trajectories in roots. *J. Exp. Bot.* **65**, 2633-2643.

**Thompson, B. J., Bhansali, R., Diebold, L., Cook, D. E., Stolzenburg, L., Casagrande, A.-S., Besson, T., Leblond, B., Désiré, L., Malinge, S. et al.** (2015). DYRK1A controls the transition from proliferation to quiescence during lymphoid development by destabilizing Cyclin D3. *J. Exp. Med.* **212**, 953-970.

**van Dam, T. J. P., Zwartkruis, F. J. T., Bos, J. L. and Snel, B.** (2011). Evolution of the TOR pathway. *J. Mol. Evol.* **73**, 209-220.

**Van Leene, J., Hollunder, J., Eeckhout, D., Persiau, G., Van De Slijke, E., Stals, H., Van Isterdael, G., Verkest, A., Neirynck, S., Buffel, Y. et al.** (2010). Targeted interactomics reveals a complex core cell cycle machinery in Arabidopsis thaliana. *Mol. Syst. Biol.* **6**, 397.

**Vandesompele, J., De Preter, K., Pattyn, F., Poppe, B., Van Roy, N., De Paepe, A. and Speleman, F.** (2002). Accurate normalization of real-time quantitative RT-PCR data by geometric averaging of multiple internal control genes. *Genome Biol.* **3**, research0034.

**Vanstraelen, M., Baloban, M., Da Ines, O., Cultrone, A., Lammens, T., Boudolf, V., Brown, S. C., De Veylder, L., Mergaert, P. and Kondorosi, E.** (2009). APC/C-CCS52A complexes control meristem maintenance in the Arabidopsis root. *Proc. Natl. Acad. Sci. USA* **106**, 11806-11811.

**Wang, D., Harper, J. F. and Gribskov, M.** (2003). Systematic trans-genomic comparison of protein kinases between Arabidopsis and Saccharomyces cerevisiae. *Plant Physiol.*. **132**, 2152-2165.

**Wang, P., Alvarez-Perez, J. C., Felsenfeld, D. P., Liu, H., Sivendran, S., Bender, A., Kumar, A., Sanchez, R., Scott, D. K., Garcia-Ocana, A. et al.** (2015). A high-throughput chemical screen reveals that harmine-mediated inhibition of DYRK1A increases human pancreatic beta cell replication. *Nat. Med.* **21**, 383-388.

**Wang, J., Song, J., Clark, G. and Roux, S. J.** (2018a). ANN1 and ANN2 function in post-phloem sugar transport in root tips to affect primary root growth. *Plant Physiol.* **178**, 390-401.

**Wang, P., Zhao, Y., Li, Z., Hsu, C. C., Liu, X., Fu, L., Hou, Y. J., Du, Y., Xie, S., Zhang, C. et al.** (2018b). Reciprocal regulation of the TOR kinase and ABA receptor balances plant growth and stress response. *Mol. Cell.* **69**, 100-112 e106.

**Wiechmann, S., Czajkowska, H., de Graaf, K., Grötzinger, J., Joost, H.-G. and Becker, W.** (2003). Unusual function of the activation loop in the protein kinase DYRK1A. *Biochem. Biophys. Res. Commun.* **302**, 403-408.

**Xie, M. W., Jin, F., Hwang, H., Hwang, S., Anand, V., Duncan, M. C. and Huang, J.** (2005). Insights into TOR function and rapamycin response: chemical genomic profiling by using a high-density cell array method. *Proc. Natl. Acad. Sci. USA* **102**, 7215-7220.

**Xiong, Y. and Sheen, J.** (2012). Rapamycin and glucose-target of rapamycin (TOR) protein signaling in plants. *J. Biol. Chem.* **287**, 2836-2842.

**Xiong, Y., McCormack, M., Li, L., Hall, Q., Xiang, C. and Sheen, J.** (2013). Glucose-TOR signalling reprograms the transcriptome and activates meristems. *Nature* **496**, 181-186.

**Yi, D., Alvim Kamei, C. L., Cools, T., Vanderauwera, S., Takahashi, N., Okushima, Y., Eekhout, T., Yoshiyama, K. O., Larkin, J., Van den Daele, H. et al.** (2014). The Arabidopsis SIAMESE-RELATED cyclin-dependent kinase inhibitors SMR5 and SMR7 regulate the DNA damage checkpoint in response to reactive oxygen species. *Plant Cell* **26**, 296-309.

**Yu, K., Shi, C., Toral-Barza, L., Lucas, J., Shor, B., Kim, J. E., Zhang, W.-G., Mahoney, R., Gaydos, C., Tardio, L. et al.** (2010). Beyond rapalog therapy: preclinical pharmacology and antitumor activity of WYE-125132, an ATP-competitive and specific inhibitor of mTORC1 and mTORC2. *Cancer Res.* **70**, 621-631.

**Zhang, Z., Smith, M. M. and Mymryk, J. S.** (2001). Interaction of the E1A oncoprotein with Yak1p, a novel regulator of yeast pseudohyphal differentiation, and related mammalian kinases. *Mol. Biol. Cell.* **12**, 699-710.

**Zhang, Z., Zhu, J.-Y., Roh, J., Marchive, C., Kim, S.-K., Meyer, C., Sun, Y., Wang, W. and Wang, Z.-Y.** (2016). TOR signaling promotes accumulation of BZR1 to balance growth with carbon availability in arabidopsis. *Curr. Biol.* **26**, 1854-1860.

**Zhao, S. and Fernald, R. D.** (2005). Comprehensive algorithm for quantitative real-time polymerase chain reaction. *J. Comput. Biol.* **12**, 1047-1064.